D2.7 Report on reliability and lifetime of semi-fabricates

WP2

Lead Partner: TNO

Partner Contributors: PCCL, EUR, G2P

Dissemination Level: Public

Deliverable due date: 30/06/2025 Actual submission date: 30/06/2025

Deliverable Version: 1.1

Funded by the European Union

Project funded by

Schweizerische Eidgenossenschaft
Confédération suisse
Confederazione Svizzera
Confederaziun svizra

Swiss Confederation

Federal Department of Economic Affairs, Education and Research EAER
State Secretariat for Education, Research and Innovation SERI

Project Acronym	MC2.0
Project Title	Mass customization 2.0 for Integrated PV
Grant Agreement n°	101096139
Call	HORIZON-CL5-2022-D3-01
Topic	HORIZON-CL5-2022-D3-01-03 Advanced manufacturing of Integrated PV
Starting Date	1 January 2023
Duration	38 months

Funded by the European Union. Views and opinions expressed are however those of the author(s) only and do not necessarily reflect those of the European Union. Neither the European Union nor the granting authority can be held responsible for them.Type equation here.

Document history

Version	Date	Comments
V0.0	09-04-2025	
V0.1		Additions from EURAC G2P testing
V0.2	19-05-2025	Additions TNO, review G2P
V0.3	29-05-2025	Contribution from PCCL added
V1.0	06-06-2025	Final Draft for internal review
V1.1	10-06-2025	Input G2P Updated for final draft internal review
V1.2	13-06-2025	Internal Review
V2.0	23-06-2025	Updated document for final submission

Executive Summary

This document contains the main deliverable for Task 2.6 (Reliability testing of semi-fabricates) within the MC2.0 project, which is a report on the reliability and lifetime of photovoltaic (PV) semi-fabricates (SFs). The term SF in this context is used to underline the semi-finished nature of these PV devices, which are meant to be supplied to manufacturers of integrated PV (IPV) for final integration into their respective products. The production of the SF would then be done by a third-party on an automated roll-to-roll (R2R) production line, referred to in the project as Mass Customization (MC) line. The MC-line has been designed to allow automated production of SFs with various designs, sizes and bill of materials (BoMs) for different applications, thus potentially offering a low-cost solution for customized IPV applications. Within the MC2.0 project, work is being done on both the development of the production process for the pilot MC-line and the most suitable design (BoM, architecture) for SFs for diverse applications. For both topics, continuous reliability testing of produced SFs is crucial, as the R2R lamination used on the MC-line poses new challenges compared to conventional sheet to sheet vacuum lamination (S2S). The results from reliability testing were in turn important input for further improvement of the process and BoM.

Within the MC2.0 project, the focus for SF design is specifically on three types of building integrated PV (BIPV) products: rooftiles, façade elements and insulated glass units (IGUs). Considering the similarities and differences in product design and resulting SF requirements, reliability testing has been separated into two categories:

- Reliability testing on generic SFs for non-transparent BIPV (presented in chapter 2)
- Reliability testing of SFs for transparent BIPV back-end products (presented in chapter 3)

For both categories of reliability testing, standard tests as prescribed by IEC61215 (Terrestrial PV modules - Design and qualification and type approval) [1, 2] and IEC61730 (PV module safety qualification) [3] were used. In particular, the climatic tests damp heat (DH) at 85°C and 85% relative humidity (RH), thermal cycling (TC) between -40°C and +85°C, and Humidity Freeze (HF) from 85°C to -40°C were performed to test SF reliability. Characterization of the SFs was performed with a combination of current-voltage (IV), electroluminescence (EL), photoluminescence (PL) measurements and visual inspection. IV measurements were performed under Standard Test Conditions (STC) of 25°C, 1000 W/m^2 intensity and AM1.5 spectrum.

Reliability testing for non-transparent BIPV – TNO, PCCL

Reliability testing for the non-transparent BIPV was performed at TNO, in collaboration with PCCL for testing of material properties (see Appendix A and Appendix B). All tests reported in chapter 2 were performed on functional PV devices or SFs, produced either in the laboratory or on the MC pilot line. The tests were performed with three main goals: shortlisting the BoM for mass-customized SFs, developing a suitable process for the MC-line and identifying the impact of storage, transport and handling on the mass-customized SFs.

Shortlisting the BoM

For the selection of most suitable BoM, reliability tests were performed on SFs produced with candidate materials. First tests were performed on S2S lamination as reference for optimal processing conditions. If S2S laminated devices passed the reliability tests, devices were produced in a laboratory R2R laminator to determine suitability of the materials for R2R lamination, identify best process parameters, and determine the reliability of the resulting devices. A baseline architecture was defined for generic SFs at the beginning of the project, which was used for the reliability tests (see section 2.1). The baseline BoM

selected for use on the MC-line production is only presented in anonymized form for confidentiality reasons. Validation tests for six different types of material are reported (section 2.1):

- **Front sheet**: Six different flexible PET based front sheets were compared in a DH test of S2S laminated devices to determine the level of moisture protection offered. This allowed identification of the most promising candidate for use during testing on the MC-line. In addition to the performance of the FS in DH, the availability and mechanical resilience also played a role in the selection. Two other ETFE front sheets have also been found to perform well in DH, but would still require further testing before replacing the current selection.
- **Back sheet**: Three PET/Alu based back sheets with lower thickness were compared to the previous state-of-the-art (SOTA) back sheet in a DH test with S2S and R2R laminated devices. This showed that thinner back sheets outperformed the previous SOTA, and a new baseline back sheet was selected with thickness similar to the front sheet to minimize mechanical stress in the stack. In a separate DH test, the same back sheet supplied with Cu-foil for back-contacting was Cu-milled and used for S2S and R2R laminated devices. The results showed no indication of compromised moisture protection after Cu-milling. This was the first step for validation of the new baseline back sheet with Cu-foil.
- **Encapsulant**: The material properties of six different polyolefin (PO) based encapsulants were characterized by PCCL and TNO. Based on the observed material properties, R2R lamination was attempted with each type of encapsulant for production of devices for DH and TC exposure. After first results, the lamination parameters for two formulations of encapsulant could be optimized to achieve the required lifetime in corresponding materials. One encapsulant could be selected from the test offering best processability and reliability. However, research on encapsulants is still ongoing as the R2R lamination step can benefit from further improvement of PO properties.
- **EVA/PET/EVA (EPE)**: For the purpose of back-contacting, the intention is to use black EPE between the cells and Cu-foil. As the first generation of the MC-line will use thin film Cu(In,Ga)Se_2 (CIGS), DH tests were performed with devices in which a layer of EPE instead of PO encapsulant was placed underneath the CIGS cells, to test chemical compatibility between EPE and CIGS. This showed the two tested EPE materials could be used in combination with CIGS PV cells, and resulted in a selection of EPE for on the MC-line.
- **Electrically Conductive Adhesives (ECA)**: For back-contacting, ECA is used on the MC-line. Three fast curing ECAs where compared in a DH and TC test of R2R laminated devices. While no significant difference was found between the ECAs in DH testing, TC showed significantly better performance of a low silver ECA. Additional tests to confirm these results are still in progress, with one of the other fast curing ECAs used as baseline material in the meantime.
- **Edge Sealant (ES)**: Three ESs were compared in a DH test of R2R laminated devices. Two of the ESs had thicknesses of 0.6 mm and were based on butyl rubber. The third ES had thickness of only 0.05 mm and was based on an undisclosed material. The latter ES performed significantly worse. The 0.6 mm edge seal with best properties for R2R processing was selected for the baseline BoM.

Developing the process for the MC line.

To establish a suitable process for R2R lamination of SFs on the MC-line, multiple runs on the line were performed using the baseline BoM, which was updated if justified by test results from the BoM validation described above. The most important processing parameters that were investigated were temperature and speed of lamination, possible prelamination strategies and preheating stages (see section 2.2). The results of DH and TC testing showed that at the current stage of development most reliable SFs could be produced by performing the full stack R2R lamination at 0.3 m/min web speed and with high pressure. Work is ongoing to further improve the process to allow higher web speeds and throughput. SFs with

current baseline BoM and processing have passed the IEC requirement of retaining 95% initial efficiency after 1000 h DH [1] (see section 2.2)

Establishing the impact of handling, storage and transport on SF reliability

As described above, SFs would in most cases need to be stored, transported and integrated after production to obtain a finished BIPV product. Hence, in addition to standard PV reliability, it is important to have better insight into the type of storage and handling the SFs can endure without losing performance or attaining visual damage. At the time of writing, two tests had been performed in this regard: an in-house built impact test combined with DH, and a scratch resistance test. The impact test showed some novel and highly flexible front sheets lost their moisture protective properties after small impact, making them less suitable for use in a SF that requires further handling and integration into products with no additional protective layers. The best performance in impact resistance was found in the front sheet currently used in the baseline BoM. The scratch resistance tests also showed very large variability between front sheets. The current baseline FS did not score best in this respect, indicating possible need for a protective layer. A first assessment of suitable materials for such a protective layer resulted in the choice for low-density polyethylene (LDPE), while other materials may be suitable for increased mechanical impact resistance, such as Polyethylene (PE) and Polypropylene (PP).

Reliability testing of SFs for transparent BIPV back-end products – EUR, G2P

The reliability testing of SFs for BIPV end-products designed for PV IGUs (in particular the Heli-ON^{TM}, a product concept developed by G2P) was performed on crystalline silicon (c-Si) based SFs already in the market. These reliability tests mainly served two purposes: to determine the performance and reliability of different c-Si SFs on the market and to determine the impact of transport, storage and handling on the performance. The reliability testing was performed in four phases.

- **Phase 1**: Tests on full Heli-ON^{TM} prototypes with 100 cycles TC. The test results showed necessity for more elaborate testing into SF reliability, which was done in phase 2.
- **Phase 2**: c-Si SFs were tested in 100 cycles TC. The results were used for improvement of the end-product design, to be tested in phase 3.
- **Phase 3**: The end-product was tested with updated design, and 18 PV arrays (each with 3 parallel SFs) were tested to get more insight into the reliability of SFs from different suppliers. These results showed large variations between SFs from different suppliers, which pointed to differences in handling, storage and transport. The effects of the latter aspects were considered in phase 4.
- **Phase 4**: A large number of samples was divided into groups for different manufacturers. The shipping methods were documented, and the performance for all SFs were measured in I-V and EL. This showed large differences. For some suppliers, evidence of cell cracking was observed. Two suppliers were found to have significantly higher power output, suggesting less damage to SFs during shipping and handling. The suppliers showing highest power also had the highest level of protection of the SFs. However, future testing would be necessary comparing the SF performance at the manufacturer location and shipping location to draw further conclusions on effects of handling and transport.

Table of Contents

List of Figures

List of tables

Abbreviations and Acronyms

[BIPV] - Building-Integrated Photovoltaics
[BoM] – Bill of Materials
[BS] – Back Sheet
[CA] – Cellulose Acetat
[CIGS] – $Cu(In,Ga)Se_2$
[cm] – Centimeter
[CN] – Carbon Nitride polymer
[Cu] – Copper
[c-Si] – crystalline silicon
[DH] – Damp Heat
[DMTA] – Dynamic Mechanical Thermal Analysis
[DSC] – Differential Scanning Calorimetry
[EBA] – Ethylene Butyl Acrylate
[ECA] – Electrically Conductive Adhesive
[EL] – Electroluminescence
[EPE] – EVA/PET/EVA
[ES] – Edge Sealant
[ETFE] – Ethylene Tetrafluoroethylene
[EVA] – Ethylene-vinyl Acetate
[FS] – Front Sheet
[HDPE] – Low Density Polyethylene
[HF] – Humidity Freeze
[G2P] – Glass to Power
[IEC] – International Electrotechnical Commission
[IGU] – Insulating Glass Unit
[I_{MPP}] – Maximum Power Point Current
[IPV] – Integrated Photovoltaics
[IV] – Current-voltage measurements
[LDPE] – Low Density Polyethylene
[MC] – Mass Customization
[MPP] – Maximum Power Point
[MWT] – Metal Wrap Through
[PA] – Polyamide
[PE] – Polyethylene
[PFAS] – Per- and Polyfluoroalkyl substances
[PET] - Polyethylene Teraphalate
[PL] – Photoluminescence
[PO] – Polyolefin
[PP] – Polypropylene
[PV] – Photovoltaics
[R2R] – Roll to Roll
[RH] – Relative Humidity
[Rs] – Series resistance
[S2S] – Sheet to sheet
[SF] – Semi-fabricate
[SOTA] – state-of-the-art
[STC] – Standard Test Conditions
[TC] – Thermal Cycling
[TGA] – Thermogravimetric Analysis
[TCO] – Transparent Conductive Oxide
[T_{MAX}] = Maximum Temperature
[T_{MIN}] = Minimum Temperature
[TPO] – Thermoplastic Polyolefins
[UV] – Ultraviolet
[V_{MPP}] – Maximum Power Point Voltage
[V_{OC}] – Open-circuit Voltage
[WP] – Work package

1 Introduction

Building-Integrated Photovoltaics (BIPV) represent a transformative approach to renewable energy integration, where photovoltaic (PV) modules are embedded directly into the building envelope. Unlike conventional PV systems, BIPV modules must not only generate electricity but also meet architectural and structural design criteria. To accommodate this dual role, the concept of Mass Customization (MC) offers a promising solution by enabling the cost-effective production of PV modules tailored to specific aesthetic and functional requirements. The project MC2.0 aims at demonstrating four different BIPV elements: a solar façade element (prototyped by Schweizer), a rooftile (Wienerberger), venetian blinds in an insulating glass unit (iWin) and a transparent window (Glass to Power, G2P in the following). All these integrated PV products rely on solar modules produced according to the concept of Mass Customization, which in this report are referred to as semi-fabricates (SFs). A SF is therefore defined as the solar laminate that is provided to the manufacturers of integrated PV products. It consists of all the components that are required to guarantee functionality and durability to the final product.

BIPV systems are exposed to varying environmental conditions and mechanical stresses, making it critical to meet stringent durability and performance standards throughout their service life. The expected lifetime of a BIPV product is clearly linked to the reliability of the SFs.

The key factors influencing the reliability of SFs are the Bill of Materials (BoM) and the processing conditions used in manufacturing. In roll-to-roll (R2R) laminated PV modules made by Mass Customization, variations in material selection, lamination parameters, and production settings can have a substantial impact on the mechanical integrity and performance stability of SFs. Furthermore, the conditions for storage, handling and transport of the SFs before their integration into the final product, and the integration process itself, can also affect the reliability of the SFs and the lifetime of the integrated PV elements.

This report describes the progress made in work package (WP) 2 (Flexible Automated manufacturing at pilot line level), task 2.6 of the MC2.0 project: Reliability testing of SFs. The report is divided into two main sections:

1. **Reliability testing on generic SFs for non-transparent BIPV**: This section focuses on SFs for end-products requiring non-transparent solar modules (i.e. the Wienerberger rooftile and the Schweizer facade element). First, the results for optimization of the BoM are reported, with detailed discussions on components such as the front sheet (FS), back sheet (BS), Polyolefin (PO) encapsulant, EVA/PET/EVA (EPE), isotropic conductive adhesives (ECAs), and edge sealants (ES). Then, the development of the lamination strategies for the MC-line process are covered. Finally, effects of handling, storage, and transport on SFs are covered, focusing on scratch and impact resistance and protective films.
2. **Reliability testing of SFs for transparent BIPV back-end products:** This section addresses reliability testing and optimization of manufacturing process parameters of SFs for transparent BIPV products (i.e. the insulating glass units made by G2P). The effects of handling, storage, and transport on the reliability of these SFs are also discussed in this section.

The reliability of SFs is evaluated through accelerated lifetime tests as described in the IEC norms 61215 [1, 2] and 61730 [3]. The selection of the test to perform was made based on the nature of the SFs (i.e. $Cu(In,Ga)Se_2$ or crystalline Si), its intended final application and the expected conditions during storage and transport. In some cases, tests with combined stress factors which are not included in the standard but relevant for the specific applications were also performed. This report offers an extensive study of the performance of SFs made for different BIPV applications and an assessment of their reliability under different stress factors.

2 Reliability testing on generic SFs for non-transparent BIPV

One of the main goals of reliability testing was to develop a generic mass customized SF that would be suitable for integration into various non-transparent BIPV products. Such a generic SF would ideally be as flexible as possible (for applications requiring shaping) while also guaranteeing electrical insulation, mechanical protection and weathering protection of the PV layers.

The tests reported in this chapter were all performed at TNO, on samples produced either in the lab or at the Mass Customization (MC) line. Nearly all tested devices had the architecture shown in Figure 1 (referred to as "baseline" in the following), with some variations in sample size and number of cells, as shown in Figure 3. There were two sets in which the architecture deviated from the baseline. For tests on back-sheet with copper (Cu) cladding (see section 2.1.2.1), the back-contacted architecture shown in Figure 2 was used. In validation tests of EPE, an important material for the back-contacting architecture, the baseline architecture shown in Figure 1 was adapted to have EPE instead of PO as the bottom adhesive between CIGS cells and back sheet.

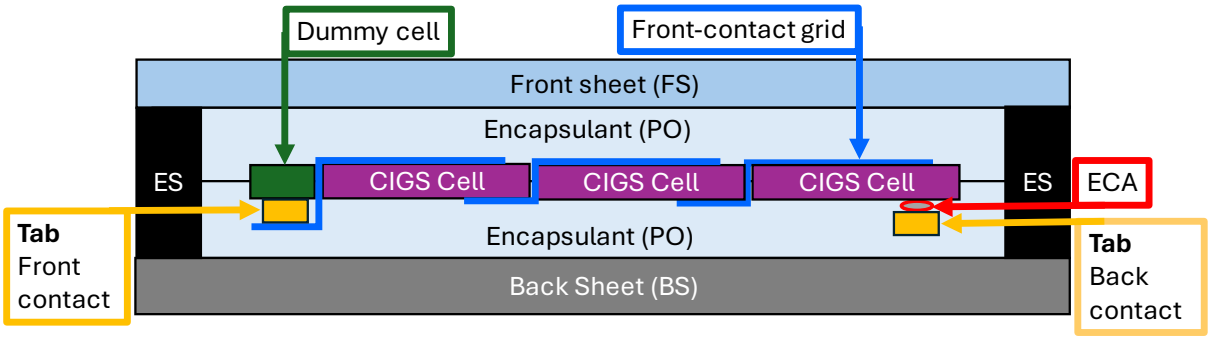

Figure 1 Baseline architecture of samples used in laboratory reliability tests for selection of BoM. The number of cells and exact shapes of the devices was varied depending on the specific test. *Note that for samples produced at the MC-line, the front-contact grid only contacted the (extended) dummy cell and not the front-contact tab. The latter was only in direct contact with the dummy cell. This is analogous to the design for back-contacting shown in Figure 2)*

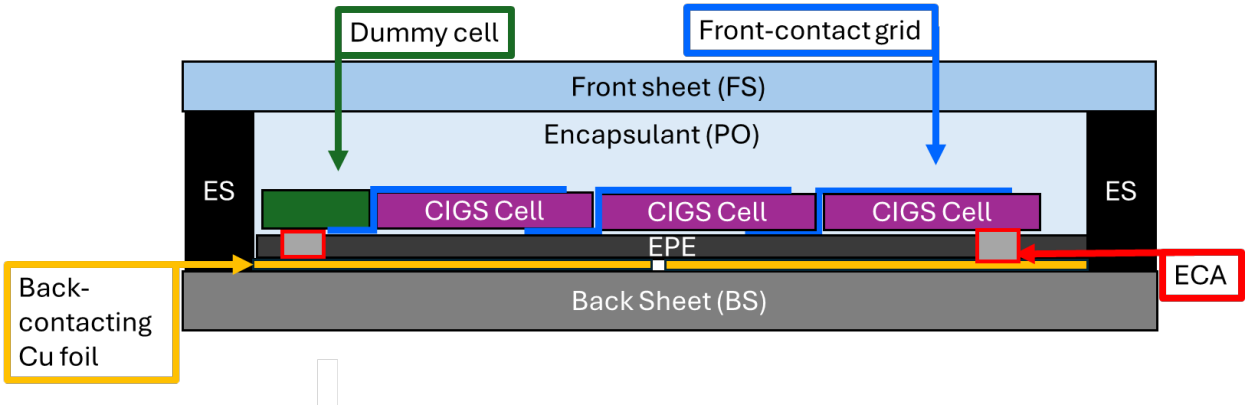

Figure 2 Architecture of back-contacted design for CIGS used in reliability tests (section 2.1.2.1).

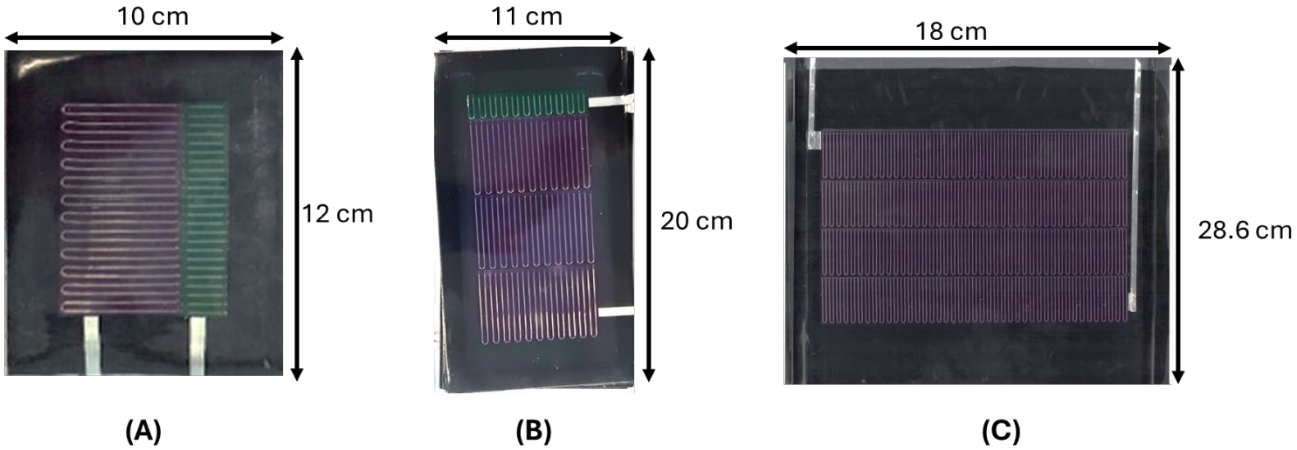

Figure 3 Pictures of reliability test samples. (A) Single cell produced in the lab. (B) Three cells in series produced in the lab. (C) Four cells in series produced on the MC-line.

In the architectures shown in Figure 1 and Figure 2, the front sheet and back sheet should sufficiently protect the active PV layers from moisture, environmental species, mechanical impact and offer electrical insulation. The edge sealant is required to prevent moisture diffusion into the SF through the encapsulant at the edges of the device between front- and back sheet. The PO encapsulant is used as adhesive between PV cell, FS, BS and tabbing. PO is chosen as opposed to more commonly used Ethylene-vinyl Acetate (EVA) to avoid the risk of acetic acid formation in case of moisture ingress. This has been observed to result in fast degradation of thin film Cu(In,Ga)Se_2 (CIGS) cells [4] which are used as baseline PV material. The ECA is used to create a reliable, electrical contact between metal interfaces. The choice for the active PV material and tabbing (flexible CIGS cells and tin plated copper tabs, respectively) were not varied, as they have been proven to give good reliability for the correct processing and BoM in past research.

The main climatic tests used for validation were Damp Heat (DH), Thermal Cycling (TC) or Humidity Freeze (HF) as prescribed in IEC61215 [1, 2] and IEC61730 [3]. The DH and TC tests were performed in an extended version (3000 hours instead of 1000 hours DH and 600 cycles instead of 200 cycles TC) to gain more insight into predominant failure mechanisms eventually limiting device lifetime. Ultraviolet (UV) testing and wet leakage and insulation testing were also performed for validation of front sheet and back sheet, but these results are not reported here.

2.1 Reliability testing to determine BoM

Validation of new candidate materials for the BoM of a generic mass customized SF was done in a step-wise fashion. First, devices were produced with the new material in S2S lamination, which can be considered the optimal process for nearly all material types (with exception of PO and ECA which needed to be specifically designed for low temperature R2R processing). Results from climatic tests on S2S laminated devices were then used as pass or fail criteria for the material, and as reference in future reliability tests on R2R laminated devices with the same material.

Once S2S laminated devices passed the relevant climatic tests, the material was used in R2R lamination of devices. Before starting reliability testing, exploratory tests were performed to determine the suitability of a material for R2R processing and appropriate processing parameters. If visually acceptable samples could be produced with the new material in R2R lamination, the produced devices underwent reliability testing. Where possible, a final validation was carried out on the MC-line, in which larger devices (shown in Figure 3 (C)) were produced for reliability tests. In the following, the main results from reliability test results are presented for a selection of suitable front sheets (section 2.1.1), back sheets (section 2.1.2), POs (section

2.1.3), EPEs (section 2.1.4), ECAs (section 2.1.5) and edge sealants (section 2.1.6). The materials showing best results in these tests were adopted for the new baseline stack, if they were also readily available in sufficient amounts. In the remainder of this report "baseline" can be considered to indicate the architecture, material choice or processing approach that was found to result in best reliability results to date. Materials that were found best performing before reliability research for MC2.0 was started is referred to as "state-of-the-art" (SOTA).

2.1.1 Front sheet (FS)

For a generic SF, a highly flexible front sheet is needed that offers sufficient moisture protection, mechanical protection and electrical insulation during product lifetime. In addition, a certain amount of mechanical resilience is required for handling in the roll on/roll off systems of the MC-line. Several climate tests have already been performed at TNO over the past years to compare different front sheets for flexible PV devices on these criteria, so a pre-selection was made to be tested for application on the MC-line.

In Figure 4, results are shown from a conventional DH test that was performed on S2S laminated devices with baseline architecture for 3 cells in series (Figure 1 and Figure 3(B)). In the test, five different flexible front sheets (labelled FS-1 to FS-5 in the following) were compared. The number of samples per configuration are shown in Table 1, and the results of the DH test are shown in Figure 4.

Table 1 Number of samples per type of FS used for the DH tests reported in Figure 4. All samples were S2S laminated.

Front Sheet	**FS-1**	**FS-2**	**FS-3**	**FS-4**	**FS-5**
DH test	5x	5x	5x	5x	5x

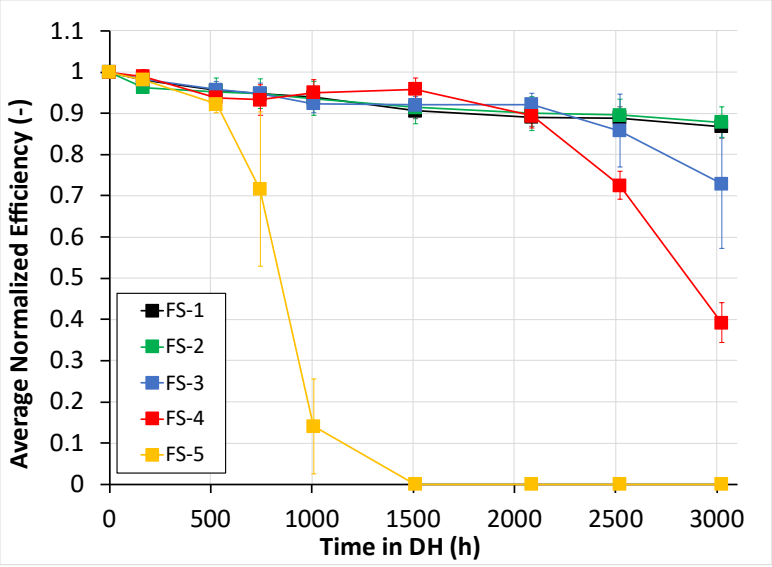

Figure 4 Average normalized efficiency as function of time in DH for S2S laminated devices with 5 different FSs. Each data point represents the average of 5 samples, the error bars indicate the standard deviation.

As clear from Figure 4, FS-5 severely underperforms compared to the other front sheets, with devices dropping below 90% of their initial efficiency after only 500 hours DH. Devices with FS-1 to FS-4, on the other hand, perform comparably up to about 2000 hours DH. Up to that point, devices for each configuration have lost approximately 10% of their initial performance, with relatively little spread between devices from the same configuration. Devices with FS-1 and FS-2 clearly show most stable performance over the course of the 3000 hours DH, losing only 13-14% relative efficiency over the course of the full test. The differences reflect

a better level of weathering protection for FS-1 and FS-2 compared to the other front sheets. Note that after 1000 hours DH, devices with FS-4 are the only devices which (barely) pass the requirement of 95% relative efficiency after 1000 hours DH [1]. However, the devices with FS-1 and FS-2 are close to passing at 94% initial efficiency after 1000 hours, while FS-3 also retains 92% initial efficiency after 1000 hours. This indicates all front sheets except FS-5 would be feasible candidates for passing the IEC requirement of DH, assuming further improvements in material and processing can increase reliability. TC tests were also performed on devices for the same selection of front sheets, these showed hardly any degradation and no distinction between front sheets.

Based on above reported DH results and material availability, FS-1 was chosen as baseline front sheet for devices produced on the MC-line, and for the reference in laboratory tests. FS-1 was also one of the best performing in mechanical impact tests combined with DH, for which the results are presented in section 2.3 (Effects of handling, storage and transport of semi-fabricates).

Work is also still ongoing to identify possibly cheaper, more flexible and ETFE-free front sheets. The topic of ETFE free front sheets is particularly important as the European Commission plans to de-phase all PFAS (Per- and Polyfluoroalkyl substances) in 2025 [5]. In Figure 5, results are shown from a first test on S2S laminated devices with the baseline front sheet (FS-1) and two ETFE-free front sheets (FS-6 and FS-7).

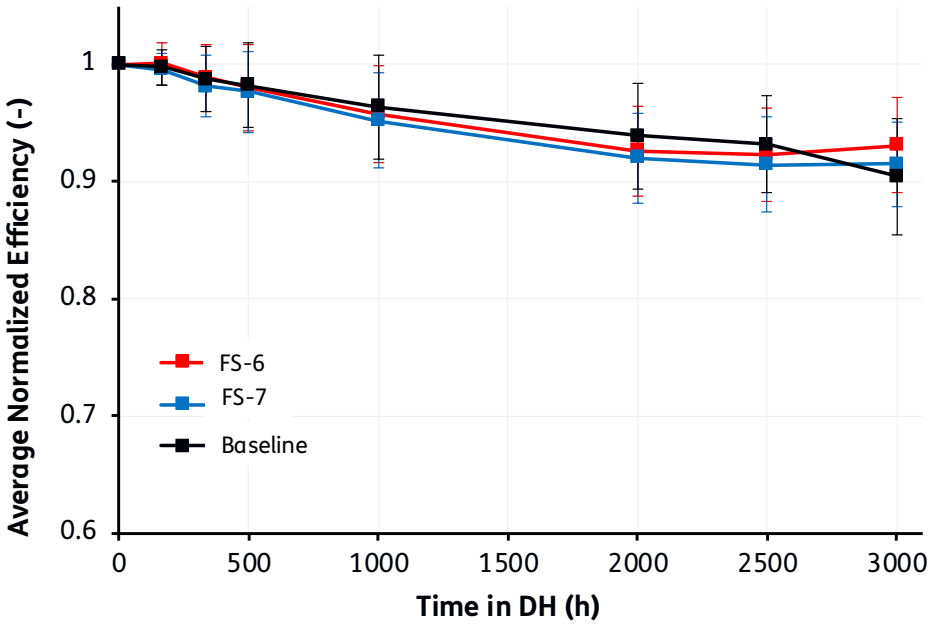

Figure 5 Average normalized efficiency as function of time in DH for S2S laminated baseline modules with different front sheets (Baseline or FS-1, and two ETFE front sheets).

As clear from the graphs in Figure 5, the devices with ETFE free alternatives FS-6 and FS-7 perform at least as well as the baseline front sheet. Moreover, on average the IEC requirement for DH is passed for each front sheet in this test. At the time of writing, no further tests had been done on these front sheets. This would still be necessary before a decision can be made about the suitability of the ETFE free front sheets for a generic SF. Important aspects that still need to be considered include resistance to fire, possible soiling, UV testing, wet leakage and insulation, scratch- and impact-resistance.

2.1.2 Back sheet (BS)

The back sheet for a generic SF requires similar properties as the front sheet, i.e. high flexibility, sufficient moisture protection and sufficient mechanical stability. Additionally, the BS thickness and material properties

directly influence the heat transfer into the stack, and therefore have an impact on the possible R2R lamination speeds for which good curing of the encapsulant can be achieved (see also section 2.2). For this reason, a thinner back sheet would not only benefit final SF flexibility, but also allow better heat-transfer and potentially faster R2R lamination speeds.

During the MC2.0 project, four different back sheets (labelled "SOTA", "BS-1", "BS-2" and "BS-3" below) have been compared in DH tests. All tested back sheets are based on an aluminium foil protected by PET layers, but each has a different total thickness. The SOTA back sheet had the highest thickness. BS-1, BS-2 and BS-3 were ordered according to decreasing thickness. In Table 2, the number of devices created per process (S2S or R2R) and for each back sheet is indicated together with the thickness of each back sheet. All devices had the baseline architecture with 3 cells in series (Figure 1 and Figure 3(B)). In Figure 6, the results of the DH experiments are shown.

Table 2 Configurations of S2S and R2R laminated samples used in the first feasibility test for thinner back sheet in DH experiments. "SOTA" was the state-of-the-art before research on the MC-line BoM started, "BS-1", "BS-2" and "BS- 3" are alternative thinner back sheets, numbered from thinnest to thickest.

Back sheet	**SOTA**	**BS-1**	**BS-2**	**BS-3**
Thickness (µm)	330	130	200	250
# S2S samples	5x	5x	5x	5x
# R2R samples	5x	---	5x	---

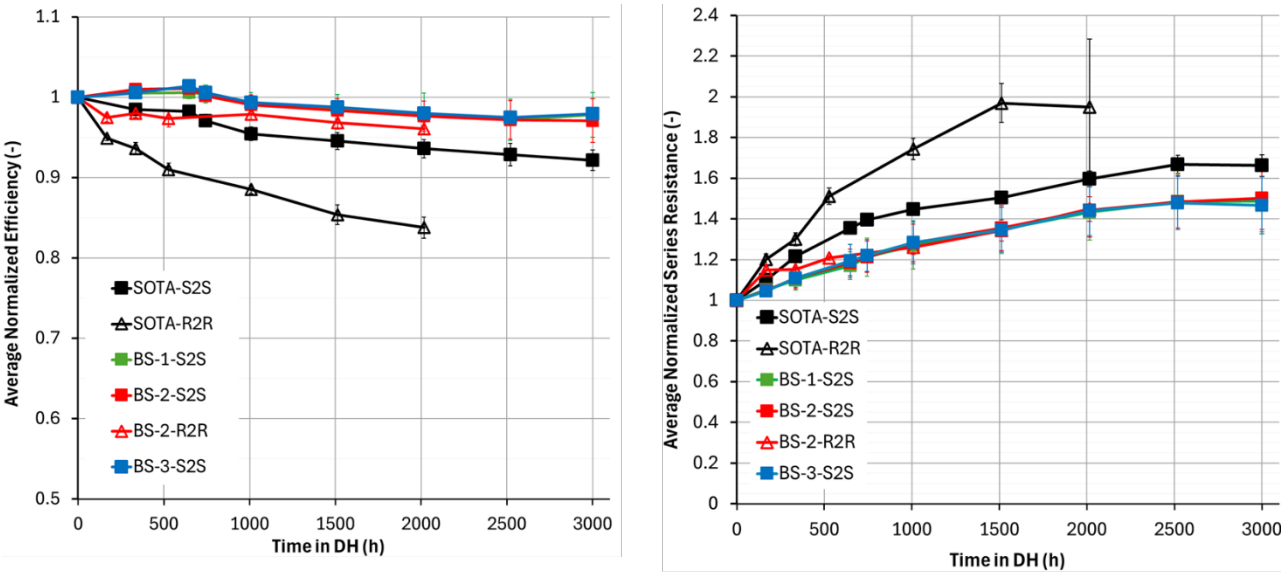

(A) **(B)**

Figure 6 (A) Average Normalized Efficiency as function of time in DH for S2S laminated (filled squares) and R2R laminated (open triangles) devices with different types of back sheet. (B) Average Normalized Series Resistance as function of time in DH. Each data point represents the average over 5 samples, the error bars indicate the standard deviation.

As clear from the graphs in Figure 6, among the S2S laminated configurations (filled squares), the configuration with the SOTA back sheet performs the worst. The configurations with thinner back sheets (i.e. with BS-1 to BS-3) on the other hand show very comparable behaviour. All three of these configurations retain over 95% of their initial efficiency after 3000 hours of DH exposure, and easily pass the IEC DH criteria. Back sheets SOTA and BS-2 were also used for R2R production of devices (open triangles). This showed an even larger difference between the two configurations. R2R laminated devices with BS-2 retain more than 95% of initial efficiency after 2000 hours DH, while devices with SOTA drop to below 85% of initial efficiency

after 2000 hours. The most important parameter responsible for the difference in efficiency between the SOTA and alternative back sheets was found to be the series resistance for both S2S and R2R processing, as shown in Figure 6(B). The hypothesis proposed to explain the observed differences is a lower amount of mechanical stress in the laminates with thinner back sheets, resulting in less problems related to contact loss over time. However, this still needs to be confirmed in further testing. All back sheets in the above test also underwent wet-leakage and insulation testing, showing sufficient performance and no significant difference between the three thicknesses in insulation before and after DH exposure. BS-2 was chosen as the new baseline back sheet, as it performed as well as BS-1 and BS-3 and best matched the thickness of the front sheet FS-1, chosen as baseline for the MC-line. A better match between back- and front sheet thickness was expected to reduce mechanical stresses after lamination and improve device lifetime. In section 2.2, results of reliability tests on samples produced on the MC-line with BS-2 and FS-1 are shown.

2.1.2.1 Cu-clad back sheet

To enable back-contacting of PV cells as envisioned for the MC-line, the supplier of BS-2 also provided material with Cu foil. A horizontal line was milled at TNO to separate front and back-contact, as shown in Figure 7(A). In Figure 7(B) and (C), the layup of the back sheet with EPE (to allow specific back-contacting with ECA dots) is also shown.

Figure 7 Pictures of Cu-clad back sheet for first feasibility test. (A) Back sheet with milled horizontal separation between “top” and “bottom” contacts, and ES along the sides. (B) Cu-clad back sheet with EPE covering part of the Cu back-contacting foil. The visible holes are for ECA placement. (C) Cu-clad back sheet covered completely with EPE after prelamination.

The EPE used in this configuration was selected based on the compatibility tests treated in 2.1.4.

Six samples were produced in S2S lamination and placed in DH to determine whether the milling had compromised moisture protection. Two samples were produced in R2R lamination to see how well the additional Cu-foil allowed lamination of the SF stack. In Figure 8, Average Normalized Efficiency, Series Resistance (R_S) and Open-Circuit Voltage (V_{OC}) are shown over the course of the DH experiment.

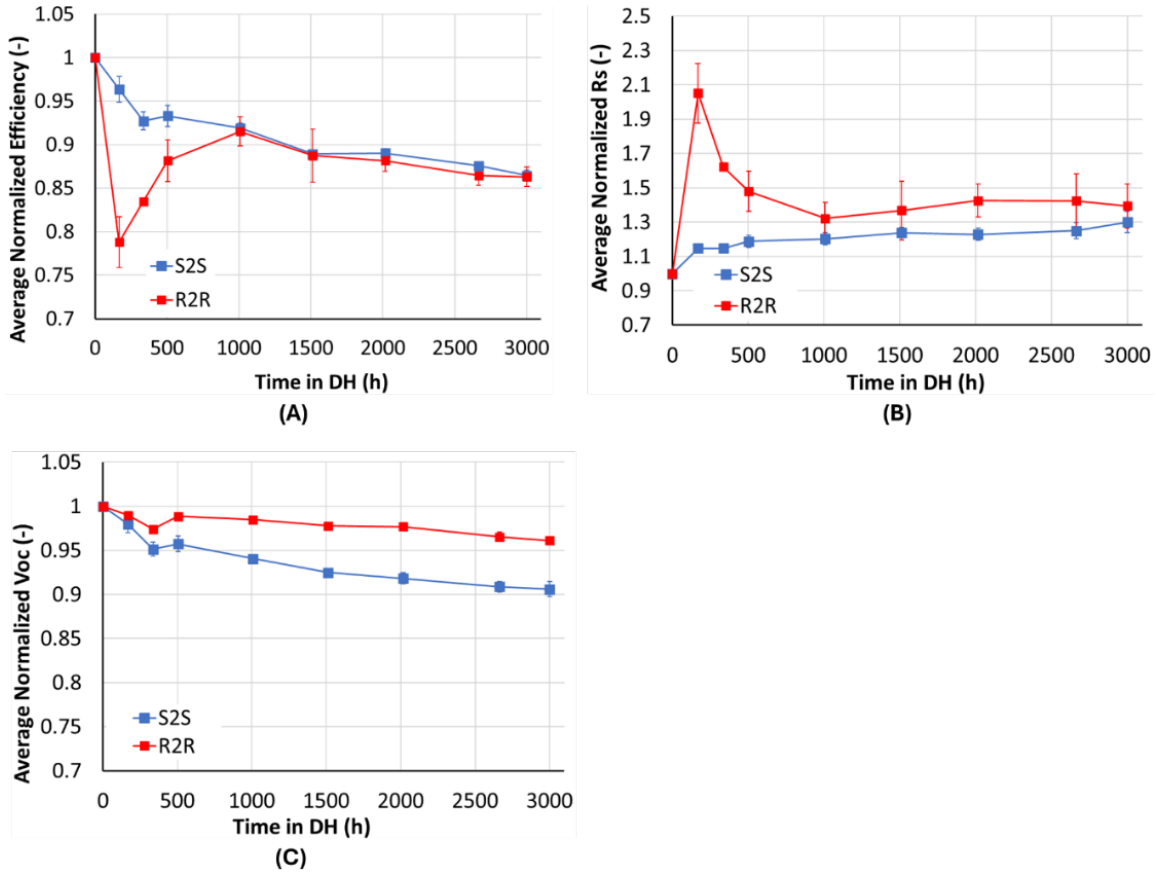

Figure 8 Results from DH experiments with devices made with Cu-clad back sheet as shown in Figure 7. For the S2S data, the average was taken over 6 samples, while for R2R data the average was taken over only 2 samples. The error bars indicate the standard deviation. The graphs show (A) Average Normalized Efficiency, (B) Average Normalized series resistance (Rs) and (C) Average Normalized Open-circuit voltage (Voc).

As clear from Figure 8(A), both S2S and R2R laminated devices show an initial drop in relative efficiency within 1000 hours of DH. This initial drop is larger for the R2R laminated than for S2S laminated devices (21% versus 7% relative efficiency loss, respectively). However, the relative efficiency of R2R devices recovers after 1000 hours DH to the same level as the S2S devices (~92% of initial efficiency). It should be noted that due to higher contact resistance, the R2R devices initially had lower absolute efficiency than the S2S devices (15% versus 17%, respectively), so that the absolute efficiencies for R2R devices were lower than those of the S2S devices in the 1000-3000 hour range in Figure 8(A). The big drop and recovery in efficiency observed for the R2R laminated devices seems to correlate to a sharp increase (to over 200% of the initial value) in R_S followed by a gradual decrease "back" to less than 150% of the initial R_S value (see Figure 8(B)). This dynamic behaviour in the R_S of the R2R produced samples suggests that the DH exposure causes mechanical stresses which are somewhat relaxed over the course of the test. The exact mechanism behind this behaviour is still under investigation.

In the S2S devices, the initial drop in relative efficiency (~5%) appears to correlate to both an increase in relative R_S (over 10% relative R_S) and decrease in relative V_{OC} (~5%). Both the increase in R_S and reduction in V_{OC} are not reversed over time in DH, and could indicate the longer heat treatment results in some kind of diffusion process or other type of material degradation, possibly in combination with some mechanical stresses. However, also for this the exact mechanisms are still topic of investigation.

2.1.3 Polyolefin (PO) encapsulant

As mentioned above, the choice for PO-based rather than EVA-based encapsulants was made early on in the development of thin film CIGS based devices at TNO, as the use of EVA was found to increase the risk of fast degradation of the transparent conductive oxide (TCO) layer due to acetic acid formation upon moisture ingress [4]. In the search for PO encapsulants suitable for R2R lamination, POs from a large number of suppliers were compared on basic material properties, as well as performance in R2R laminated PV devices under climate tests. The results of material level testing, performed partly at PCCL and partly at TNO, are reported in Appendix A. Here, the results of reliability tests (DH and TC) on devices produced with different types of PO (labelled PO-1 to PO-6) are reported. The devices had the baseline architecture with single cell configuration (Figure 1 and Figure 3). Only devices produced with R2R lamination are reported, as the POs needed to be tested specifically for R2R lamination. The results are shown in Figure 9.

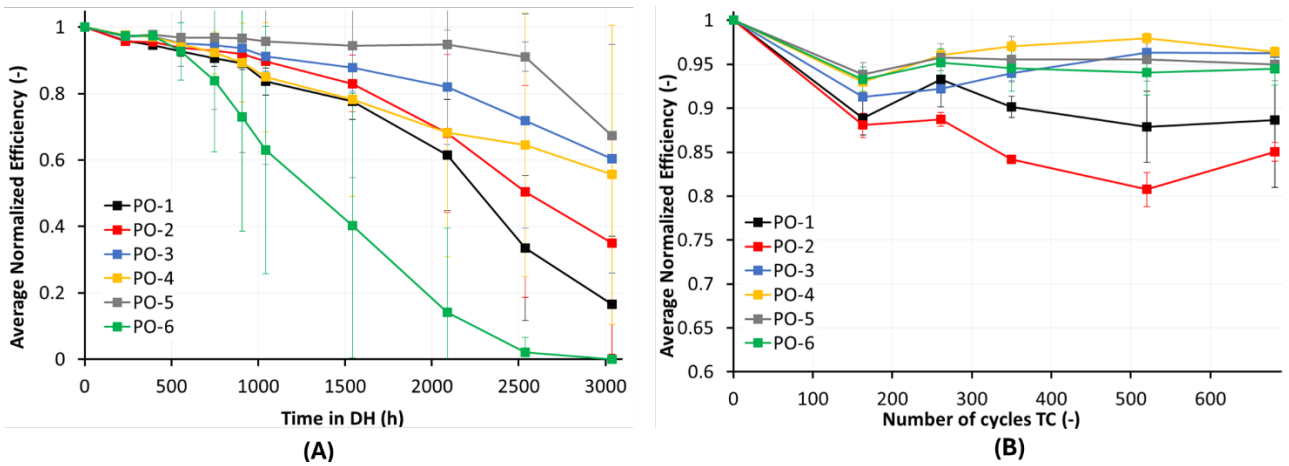

Figure 9 Average Normalized Efficiency of R2R laminated devices with 6 types PO as function of time in test. (A) Results from DH test. Each data point represents the average taken over 5 devices. (B) Results from TC test. Each data point represents the average taken over 3 devices. The error bars indicate the standard deviations.

The results from the R2R-DH test shown in Figure 9(A) show large differences in performance evolution over time for the different PO configurations and a large spread in sample performance per configuration. This reflects relatively low reproducibility in sample reliability for R2R lamination, in particular for PO-2, PO-4 and PO-6. The configuration with PO-5 performs best, and is the only configuration for which the devices retain over 95% of their initial performance after 1000 hours DH (thus passing the IEC requirement for DH). However, PO-5 performed worst in creep tests (Table 12 in Appendix A). The configuration with PO-6 performs worst, degrading to just above 60% initial efficiency after 1000 hours DH. The performance evolution for the other configurations is much closer together, and the relative efficiency after 1000 hours DH varies between 84% (PO-1) and 91% (PO-3).

The results of the R2R-TC test presented in Figure 9(B) show configurations PO-1 and PO-2 lose most performance (~12% in relative efficiency) over the first 150 cycles TC. While the relative performance for configurations PO-1 and PO-2 remains lower than for the other configurations over the course of the entire TC test, configuration PO-1 shows a recovery from 88% to 93% of initial efficiency between 150 and 250 cycles, resulting in overall worst performance for configuration PO-2. The devices with PO-3 also show a relatively large drop in the first 150 cycles TC (9% of their initial performance), but show gradual recovery over the rest of the TC test, resulting in a similar relative performance after 680 cycles as configurations PO-4, PO-5 and PO-6. For the best performing configurations PO-4, PO-5 and PO-6, the devices barely underperform for the IEC requirement of 95% of initial efficiency after 200 cycles TC, reaching between 93% (PO-4) and 94% (PO-5) of initial efficiency after 150 cycles. The performance of devices with PO-4 also recovers to more than 95% of initial efficiency after 680 cycles TC. The fluctuations in performance as seen

in all configurations have been observed more frequently in R2R laminated samples, and can usually be ascribed to unstable electrical contacts.

Based on these climatic test results and the creep test results reported in Appendix A, PO-3 was chosen as the baseline material for use on the MC-line. However, further optimization of R2R processing for PO-1 and PO-5 was found to lead to a significant improvement in performance stability, as shown in Table 3. Hence, research into alternative POs and optimized processing parameters is still ongoing.

Table 3 Average Normalized Efficiencies for devices produced with optimal R2R lamination settings compared to results shown in Figure 9 at 1000 h DH and 300 cycles TC.

	Average Normalized Efficiency	
Climatic test:	**1000 h DH**	**300 c TC**
PO-1	0.84	0.90
PO-1, Optimized	0.93	0.93
PO-5	0.96	0.96
PO-5, Optimized	0.96	0.98

2.1.4 EVA/PET/EVA (EPE)

As mentioned in the introduction of this chapter, EPE is an important material in the back-contact design shown in Figure 2. For mass customized SFs based on CIGS, it was first necessary to determine whether available EPEs were chemically compatible with the CIGS cell stack. Two EPEs from different suppliers (EPE-1 and EPE-2 below) were used as replacement for the bottom PO layer shown in the baseline architecture in Figure 1. All devices in the test were S2S laminated. The results from the DH test are shown in Figure 10. PL and EL images of one of the samples from each configuration are shown in Figure 11.

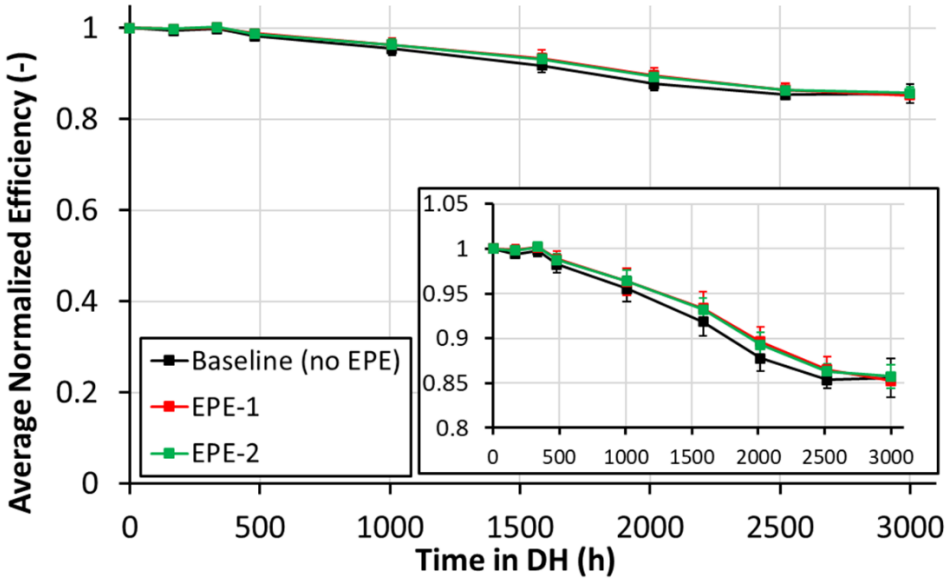

Figure 10 Average Normalized Efficiency as function of time in DH for three sample configurations: baseline without EPE (black line), EPE-1 (red line) and EPE-2 (green line). The inset in the bottom-right of the graph shows a zoomed-in version of the same graphs. Each data point represents the average taken over 5 samples. The error bars indicate the standard deviations.

As clear from the DH results shown in Figure 10, there was hardly any spread between the three different configurations. In the inset, the relative efficiency of the baseline set without EPE can be seen to drop below that of the EPE-1 and EPE-2 sets between 1000 and 2500 h DH. However, it can also clearly be seen that each configuration passes the 1000 hours DH with over 95% of initial efficiency, indicating all configurations pass the IEC criteria for DH. The spread between samples for each configuration is also very low, indicating very high reproducibility in quality. The main failure mode was found to be slight loss in V_{OC} and moderate increase in R_S, which has been commonly seen in S2S laminated devices that underwent DH testing. The PL and EL images shown in In Figure 11 are in line with this type degradation.

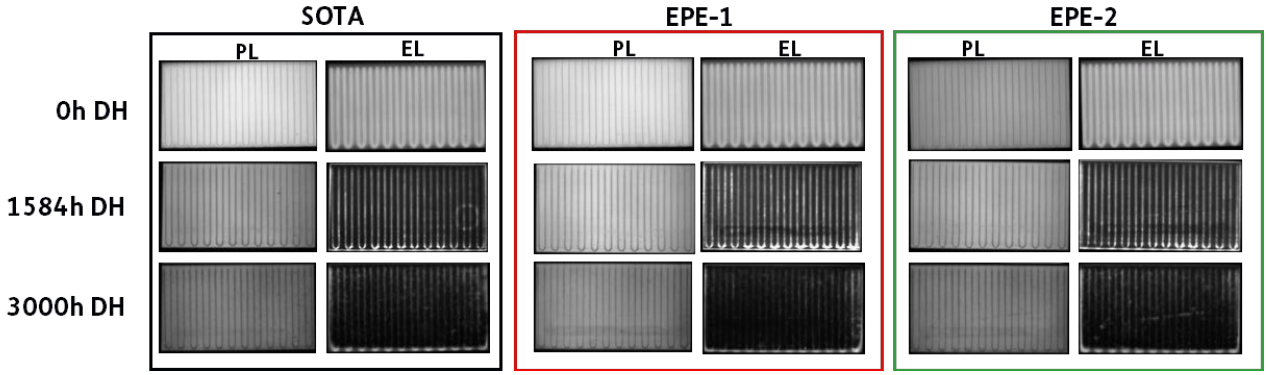

Figure 11 PL (left columns) and EL (right columns) images for one of the tested devices from each configuration at 0 h DH (top row), 1584 h DH (middle row) and 3000 h DH (bottom row). Note that all samples behaved very comparably in each configuration, so that samples shown here can be considered representative of the other samples in the set.

In Figure 11, the PL and EL images are shown for one of the samples that was found representative of the behaviour of the entire set. For each configuration, the PL signal gradually decreases between 0 h and 3000 h, reflecting some loss in V_{OC}. This appears to indicate some degradation in the active material, for which the precise reason is still unknown. The EL images mostly show an increasing contrast between wires and edges of the cell over time, reflecting the increase in R_S. As the degradation for the baseline configuration appears exactly the same as the degradation in the EPE-1 and EPE-2 configurations, the use of EPE with CIGS does not appear to pose any issues of chemical compatibility. For the back-contacted design, EPE-1 was chosen as baseline material, as it had the best adhesion of the two EPEs.

2.1.5 Electrically Conductive Adhesives (ECA)

As mentioned above, in addition to EPE, ECAs are a key material in the back contacted architecture in the MC line shown in Figure 2. ECAs can usually be applied as pastes (e.g. by dispensing), but then require a thermal treatment to be cured and become conductive. Due to the low thermal budget available in R2R lamination, it is important to have ECAs with fast curing properties. In Figure 12, results are shown from the comparison of R2R laminated devices with baseline architecture shown in Figure 1 in the single cell configuration shown in Figure 3(A) with three different types of fast curing ECAs (labelled ECA-1, ECA-2 and ECA-3). ECA-3 had a lower silver (Ag) content than ECA-1 and ECA-2, and other conventional ECAs. This configuration was added to the test to investigate the feasibility of reducing Ag content for more sustainability and lower material costs. One set of CIGS based devices was made without any ECA as “worst case” reference.

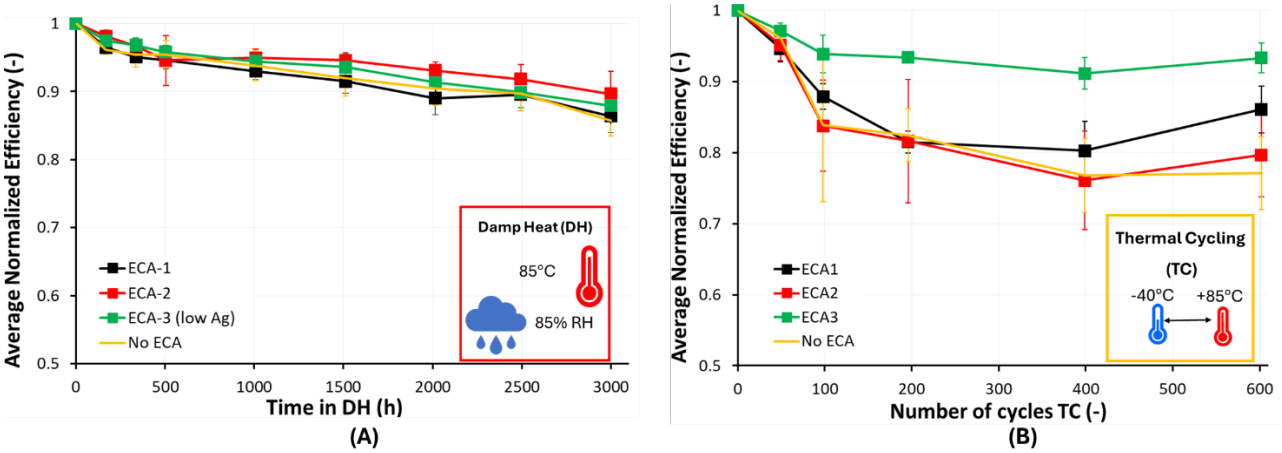

Figure 12 Average Normalized Efficiency of R2R laminated devices with variation in ECA, as function of time in (A) DH and (B) TC. Each data point in the graphs represents the average over 5 samples in (A), and the average over 3 samples in (B). The error bars show the standard deviation.

The DH results shown in Figure 12(A) show no statistically significant difference between the four configurations over the course of the test. After 1000 hours DH all configurations retain approximately 94% of initial efficiency, indicating for each ECA and even the configuration without ECA, the DH requirement according to IEC is most likely achievable with further process and design optimization. After 3000 hours DH, a loss of approximately 10% initial efficiency is observed for each configuration. This shows the ECA does not play an important role in the device reliability in DH for this architecture. In the TC results (Figure 12(B)), on the other hand, a clear difference is observed between samples with ECA-3 (i.e. the low Ag formulation) and all other variations. The samples without ECA and with ECA-2 show comparable behaviour, with ~20% loss of average normalized efficiency after the full 600 cycles TC. Samples with ECA-1 roughly follow the same trend up to 400 cycles, but due to recovery in the last 200 cycles the overall loss after 600 cycles is only ~15% relative efficiency on average. Samples with ECA-3 show a loss of just ~7% on average. These results suggest ECA-3 results in a better adhesion between the back-contact tab, and the back side of the CIGS cell. This could be a result of the lower Ag content, resulting in relatively more “adhesive”. However, more research is ongoing to identify the exact reason for different behaviour of ECA-3 in TC.

The same ECAs are being compared in DH and TC tests of R2R laminated samples with back-contacted MWT Si cells. Here again, BS-2 with Cu-cladding was used (see Figure 13).

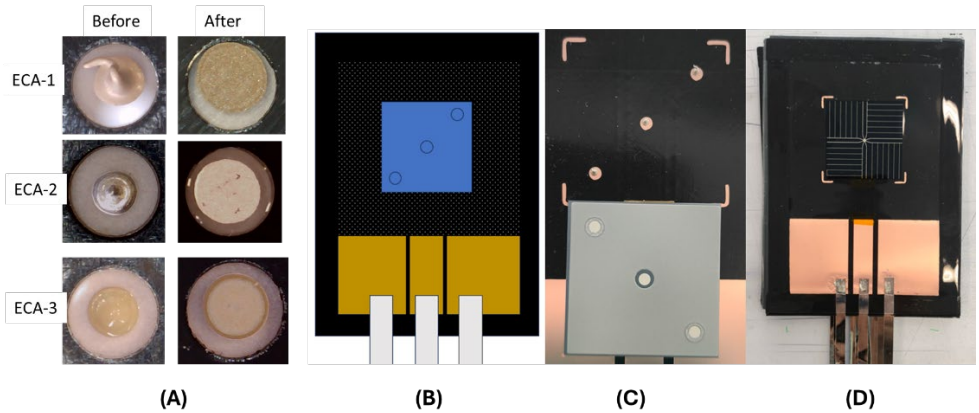

Figure 13 (A) Pictures of ECA dots for ECA-1, -2 and -3 before (left column) and after R2R lamination, for the optimal dispensing conditions. (B) Schematic of the architecture of the back-contacted samples with (cut) MWT Si cells contacted with two back-contact tabs and one front-contact tab. (C) Picture of Cu-clad back sheet covered with patterned EPE to allow back-contacting of MWT Si cell (folded down onto the contact strips). (D) Picture of the final sample with MWT Si cell.

Figure 13(A) shows the shape of droplets obtained for each type of ECA after optimized dispensing, before and after R2R lamination. To obtain the optimal results, optical images were taken to measure the spreading of the paste after dispensing different volumes. Once the right settings for dispensing were found for each ECA, back-contacted mini-modules were prepared using a MWT silicon wafer cut to a size of 3.9x3.9 cm^2. Each cell has 3 contact points (2 for the positive polarity, one for the negative) in which the ECA was applied (see Figure 13(B-D)). The samples were then placed in a climate chamber for DH and TC testing. The climatic tests were not yet finalized at submission of this deliverable.

2.1.6 Edge Sealant (ES)

As mentioned in section 2.1, edge sealant was used around the perimeter of the devices to avoid moisture ingress from the sides (i.e. between the FS and BS in Figure 1). A comparison was made between three edge sealants (labelled ES-1 to ES-3 below). To determine which of the three edge sealants was most promising for use in R2R lamination and which settings would be most suitable, Dynamic Mechanical Thermal Analysis (DMTA), thermogravimetric analysis (TGA), differential scanning calorimetry (DSC) analysis and peel testing was performed before and after lamination (see Appendix B). For ES-1 and ES-2 it was known that they were based on butyl rubber, while for ES-3 the base material was undisclosed. With the results from the material tests the most promising processing settings in R2R lamination were found. These were then used to create samples for reliability testing with baseline architecture shown in Figure 1, with the single cell configuration shown in Figure 3. The results of the DH test are shown in Figure 14.

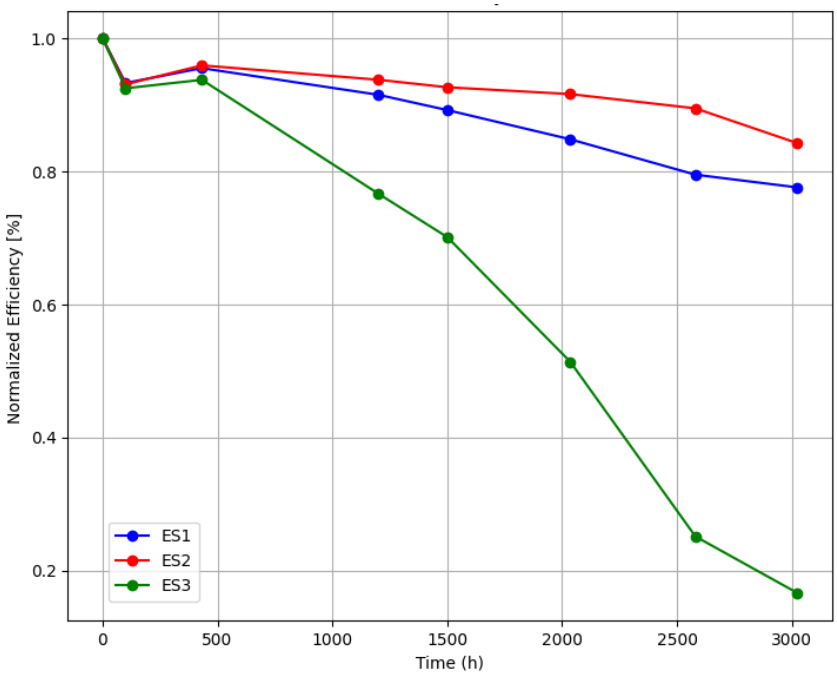

Figure 14 Results of DH test on R2R laminated devices with baseline architecture with variations in ES. Each data point represents the average taken over 5 samples.

The DH results show a very large difference in performance between ES-1 and ES-2 on the one hand and ES-3 on the other hand. The devices created with ES-3 drop below 95% of their initial efficiency within 200 hours of DH. After 3000 hours, the relative efficiency has dropped steadily to below 20% of the initial performance. The early failure in devices with ES-3 was expected to be due to its relatively low thickness (0.05 mm versus 0.6 mm) which may have resulted in insufficient pressure on the sides of the produced samples for good

sealing, or excessive mechanical stress in the devices resulting in gradual 'opening' of the edges. The evolution in relative efficiency for ES-1 and ES-2 is more similar, with overall loss of approximately 22% relative efficiency for ES-1 and 15% relative efficiency for ES-2 after 3000 hours DH. In combination with observed better malleability of ES-2 in the relevant process window, ES-2 was chosen as the most promising material.

2.2 Development of MC-line process

Optimization of the MC-line process naturally needed to be done on the MC-line itself. To restrict the amount of variables in process optimization, a baseline BoM was selected beforehand, based in part on the test results presented in the previous section. As the research to select optimal BoM and optimize the MC-line process were being performed in parallel during the project, the BoM used in test devices from the MC-line also varied over time. However, the baseline architecture shown in Figure 1 was always used (with different choices of materials), with sample design as shown in Figure 3(C).

2.2.1 Lamination strategies

As mentioned in previous sections, one of the main challenges in processing with the MC-line is to achieve sufficient heat input during the short R2R lamination process. The thermal budget highly depends on the stack thickness, (specifically the thickness of materials between rollers and encapsulant layers) and the speed of the web. Choice of thicker materials in the BoM will lead to slower heat dissipation into the encapsulant layers, while higher web speed leads to less time for heat dissipation and lower maximum temperature reached. Of course, the web speed not only influences the heat dissipation but also the throughput of the line, resulting in a trade-off between throughput and total heat input achieved.

To establish the most suitable lamination speed to work with on the current generation of the MC-line for the chosen BoM, the temperature at cell position was monitored with a thermocouple for R2R lamination at three different web speeds: 0.3 m/min, 0.6 m/min and 0.9 m/min (see Figure 15(A)). The exact temperature and time in the resulting temperature profiles are not shared for confidentiality reasons. Devices produced at each of the aforementioned speeds were also placed in DH testing, with results shown in Figure 15(B).

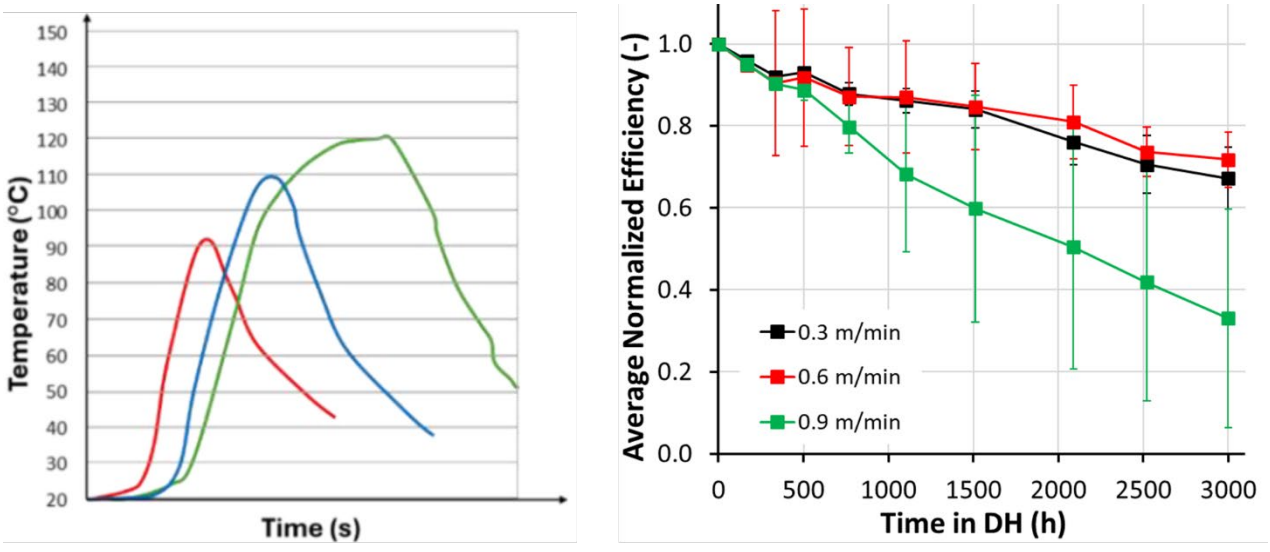

Figure 15 (A) Temperature profiles at cell position during R2R lamination at 0.9 m/min (red curve), 0.6 m/min (blue curve) and 0.3 m/min (green curve). (B) DH test results of devices produced at 0.3 m/min (red data points), 0.6 m/min

(black data points) and 0.9 m/min (green data points). Each data point represents the average efficiency over 5 samples from the same set.

As clear from Figure 15(A), the temperature peak reached is 90°C, 110°C and 120°C web speeds of 0.9 m/min, 0.6 m/min and 0.3 m/min, respectively. Meanwhile, the breadth of the temperature peak also significantly increases for lower web speeds, resulting in much higher temperature budget as web speed is reduced. As clear from the Figure 15(B), the samples that received the lowest thermal budget (i.e. were laminated at 0.9 m/min) show the fastest performance degradation in DH, with a 30% drop in relative efficiency in the first 1000 hours of exposure. The devices produced at 0.3 m/min and 0.6 m/min, on the other hand, show a much slower degradation. This clearly demonstrates the inverse relationship between R2R speed and device reliability for speeds higher than 0.6 m/min. Note that while the average relative efficiency is similar for devices produced with web speeds of 0.3 m/min and 0.6 m/min, the spread is significantly higher for the latter case. Hence, for further optimization 0.3 m/min was chosen as baseline processing.

To gain more insight into the interfaces that play the biggest role in the reliability for low heat input, a test was performed comparing three different pre-lamination strategies: (i) Prelamination of cells, tabs and ECA ("Cells+Tabs"), (ii) prelamination of only the CIGS cells ("Cells only) and (iii) no prelamination at all. For each variation, 8 samples were produced at the MC-line and tested in DH. The results are shown in Figure 16.

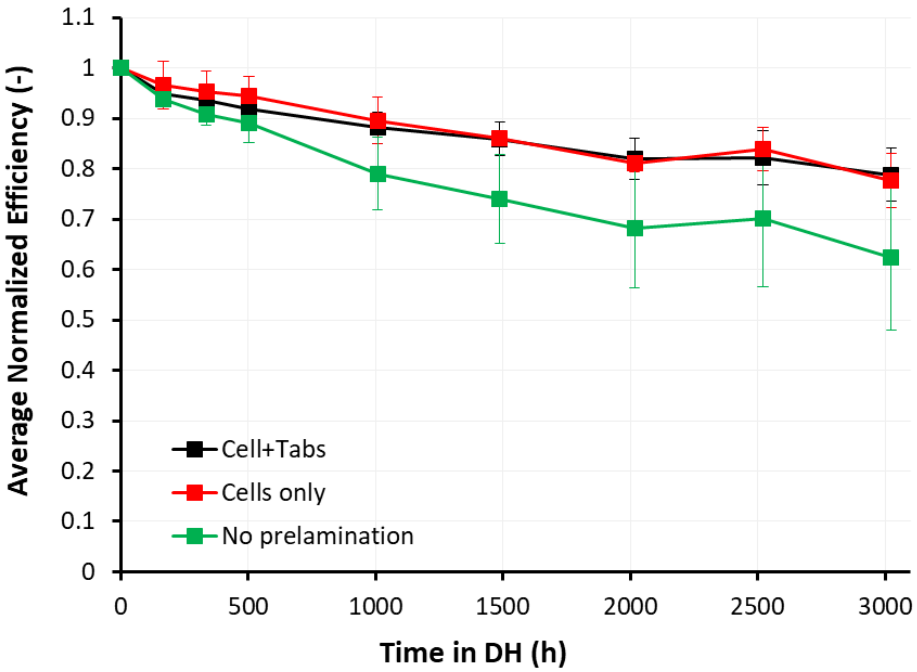

Figure 16 Average Normalized Efficiency as function of time in DH for devices laminated at the MC-line with prelamination of either cells, tabbing and ECA (black line), only cells (red line) or no prelamination at all (green line). All samples had the architecture as shown in Figure 1 and Figure 3(C). Each data point represents the average over 8 samples for the Cells only and No prelamination. In the Cell+Tabs configuration two of the produced samples failed due to production error, so only 6 samples were taken into account. The error bars indicate the standard deviation.

As clear from the DH results, the devices with prelaminated cells behave almost exactly the same as devices with prelaminated cells and tabbing, while the devices without any prelamination show fast degradation towards 80% of initial efficiency after 1000 hours DH. This shows the most important interface limiting device reliability in case of insufficient heat input is the adhesive layer on top of the front contact wiring in the commercial CIGS cells used. This thin adhesive/PET/adhesive layer needs to be melted and pressed together

for good contact, and most likely does not reach a high enough temperature for long enough with R2R lamination only.

Another attempt at improving the final lamination quality was made by applying pressure to the rolls during the R2R process (in the results above, the only pressure was due to the weight of the top role). The additional pressure in the R2R processing promotes the fixation of the adhesive layers. An experiment was performed in which devices were R2R laminated in the lab at two different pressures ("low" and "high" in the following). As reference, they were compared to S2S laminated devices. All devices had baseline architecture with the single cell configuration (Figure 1 and Figure 3(A)). Per configuration, 20 samples were produced, 10 of which were placed in DH and 10 in TC. The number of samples per configuration and test are also summarized in Table 4. The results from the climatic tests are shown in Figure 17, with DH results presented Figure 17(A) and TC results presented in in Figure 17(B). At the time of writing, the DH test had reached 1500 hours DH and the TC test had reached a 400 cycles. However, the test will be continued for 3000 hours and 600 cycles as presented in previous results.

Table 4 Number of samples produced in R2R at low pressure ("Low P") and high pressure ("High P"), and in S2S, for both DH and TC experiments.

	S2S	**R2R Low P**	**R2R High P**
DH	10x	10x	10x
TC	10x	10x	10x

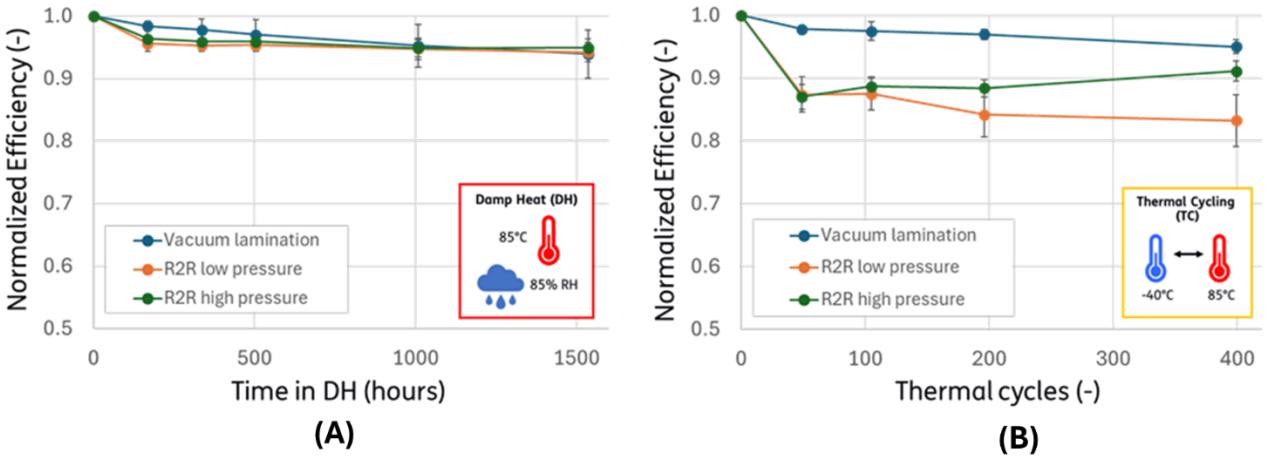

Figure 17 Normalized Efficiency as function of (A) time in DH and (B) cycles in TC for devices produced in S2S lamination (blue lines) R2R lamination at low pressure (orange lines) and R2R lamination at high pressure (green lines). Each data point represents the average over 10 devices. The error bars indicate the standard deviation.

As clear from Figure 17(A), both R2R configurations show a large initial drop in relative efficiency at 150 hours DH, after which the efficiencies stabilize. The initial drop in the S2S configuration is lower, resulting in higher relative efficiency up to 1000 hours DH. However, all samples pass the 95% initial efficiency at 1000 h DH criteria. At 1500 hours there is no longer a statistical difference between the results of R2R and S2S vacuum lamination. Overall, these DH results show that the level of moisture protection achieved with R2R lamination can be comparable to the level of moisture protection achieved with the S2S benchmark lamination.

In the TC results shown in Figure 17(B), however, a clear difference is visible between the 3 configurations. Once again, an initial drop is observed for both R2R pressures after the first 50 thermal cycles. The performance then stabilizes and even slightly improves over time for the R2R lamination performed at high pressure. For the S2S laminated samples, a steady decrease is observed, although the relative efficiency

always remains above the samples R2R laminated at high pressure. The devices R2R laminated at low pressure perform the worst, which is clearly visible from 200 and 400 cycles TC. Hence, the increased pressure during R2R lamination indeed appears to be beneficial for the mechanical stability in the produced devices. However, while the S2S laminated devices reach the 95% initial efficiency after 200 cycles, this is not the case for either R2R laminated configuration.

After implementing the above improvements to the processing in the MC-line, SFs were produced showing excellent reliability in accelerated lifetime tests. Figure 18 below shows the results of the DH test in which 3 variations were tested with different bill of materials (the baseline BOM, one with an alternative front sheet and one with an alternative encapsulant).

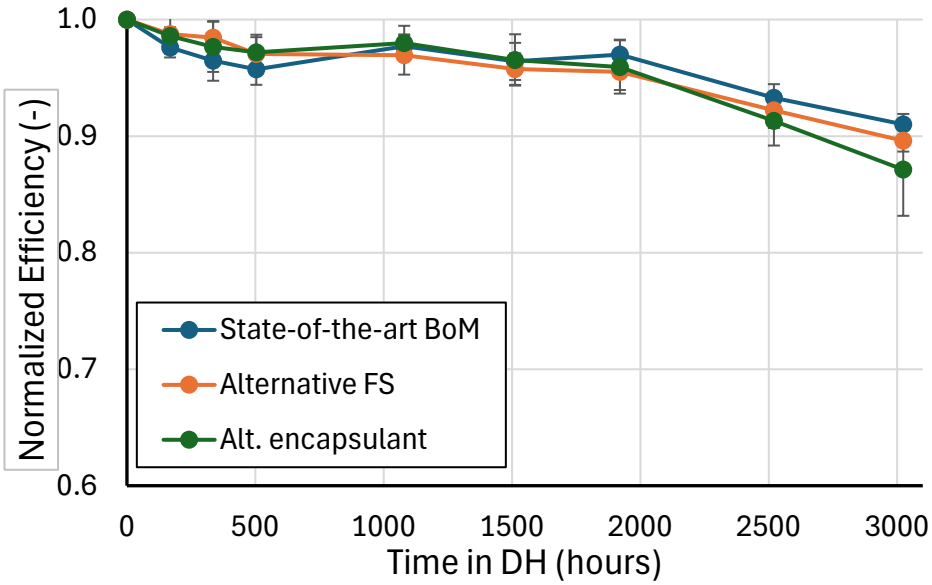

Figure 18 Normalized Efficiency as function of time in DH for 3 configurations of MC-line devices, all produced with the improvements to R2R lamination processing. Each data point represents the average taken over 5 samples. The error bars indicate the standard deviations.

All variation show very similar behaviour in DH, with the baseline BoM showing slightly better performance than the other variations. Importantly, all the samples show a loss of performance of less than 5% after 2000 hours in DH, therefore passing the requirement of the IEC 61215.

The baseline BoM was also tested in the TC and HF tests, and the results are shown in Figure 19(A) and Figure 19(B) below, respectively. In TC the devices show an initial drop in normalized efficiency of almost 15%, followed by recovery. This is in line with the results shown in Figure 17(B) above. The test is currently still in progress, and will be continued up to 600 cycles TC. The HF test shows a drop of less than 5% during the first 10 cycles, and it therefore passes the IEC 61215 requirements. This test will also be extended to 30 cycles, to assess the long term reliability of the SFs. Overall, the results from accelerated lifetime tests performed are very promising and suggest that mass customized SFs are close to certifiable.

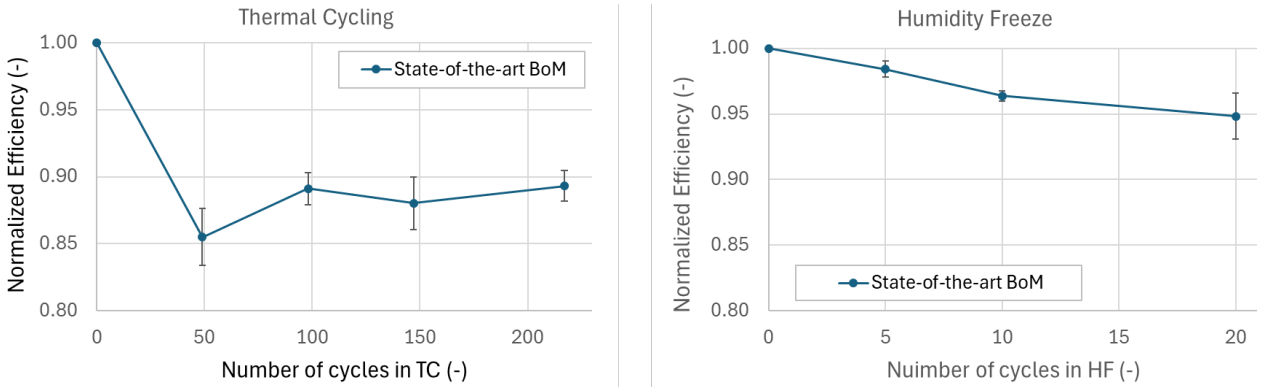

Figure 19 Average Normalized Efficiency as function of number of cycles (A) TC and (B) HF. In both tests, MC-line SFs were made with the optimized processing settings discussed above. Each data point in the graph represents the average over 5 samples. The error bars indicate the standard deviation.

In order to better understand the behaviour observed in the TC (in particular the drop and recovery in efficiency), EL imaging was performed on all the samples used in this test, at different stages of the test. The images for up to 100 cycles TC are shown in Figure 20. These show the appearance of dark areas at the edges of the CIGS cells after 49 cycles. While some dark edges are still present at 98 cycles, they have clearly reduced in severity.

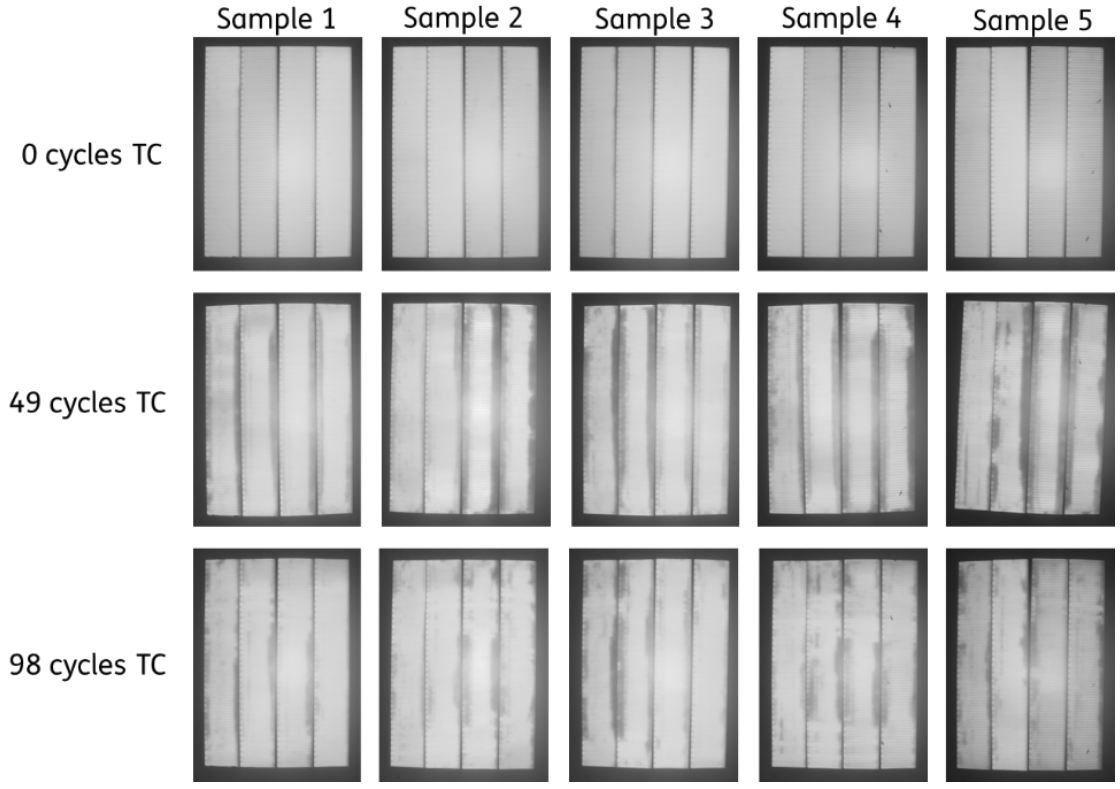

Figure 20 EL images taken for the samples produced on the MC-line for the TC test shown in Figure 19(A), for 0, 49 and 98 cycles TC (i.e. where a sudden drop and recovery is most visible in the normalized efficiency graph). The dark bands visible at 49 and 98 cycles TC indicate contact problems between the interconnections of the CIGS cells.

These dark areas indicate contact issues between the (shingled) CIGS cells. Most likely, delamination occurs at the overlap (interconnection) between the CIGS solar cells. The partial recovery of delamination after 98 cycles visible in Figure 20 would then explain the improvement in relative efficiency. The underlying

mechanism for these changes are still under investigation, but the current hypothesis is that the R2R lamination builds in certain mechanical stresses, which can be released gradually in climatic testing.

2.3 Effects of handling, storage and transport of semi-fabricates

In the mass customization concept, SFs will somehow need to be stored after production and transported to the location where they are to be integrated into the final product. To guarantee nameplate performance and reliability to a potential end-product owner buying a mass customized SF, guidelines will need to be given about correct type of storage (e.g. at which temperature and moisture level and for how long) as well as possible restrictions of handling (minimum radius of curvature for bending, maximum weight loading at different locations) etc. In section 2.3.1, the results are reported from two tests performed at TNO to determine impact and scratch resistance of SFs with different BOMs. In section 2.3.2, the results from a first assessment by PCCL of potential protective foils to be used for SFs are shown.

2.3.1 Scratch and impact resistance of mass customized SFs

For testing SF resilience to mechanical impact, an in-house built “ball-drop” test was performed, consisting of a tube guiding a small ball towards the sample for reproducible impact (see Figure 21).

Figure 21 Close-up view of one of the samples from the DH + Impact tests undergoing an impact with the in-house built “ball drop test”.

This impact test was performed on devices with baseline architecture shown in Figure 1 with 3 cells in series (Figure 3(B)), produced with four different front sheets (FS-1, FS-2, FS-3 and FS-4* below). An overview of the samples per configuration is also shown in Table 5. The labelling of FS-1 to FS-3 is in agreement with the DH test on front sheets reported in section 2.1.1 (i.e. FS-1 to FS-3 represent the same front sheets in both tests). FS-4* is a front sheet based on FS-4, but with slight improvements by the supplier. The impact tests was performed directly after sample production, after 1000 hours DH and after 2000 hours DH, each time on a different cell. The results from DH testing are shown in Figure 22, with the different moments of impact indicated by the red-dashed lines.

Table 5 Samples per configuration tested in the ball-drop + DH test

Front Sheet	**FS-1**	**FS-2**	**FS-3**	**FS-4***
S2S laminated	5x	5x	5x	5x

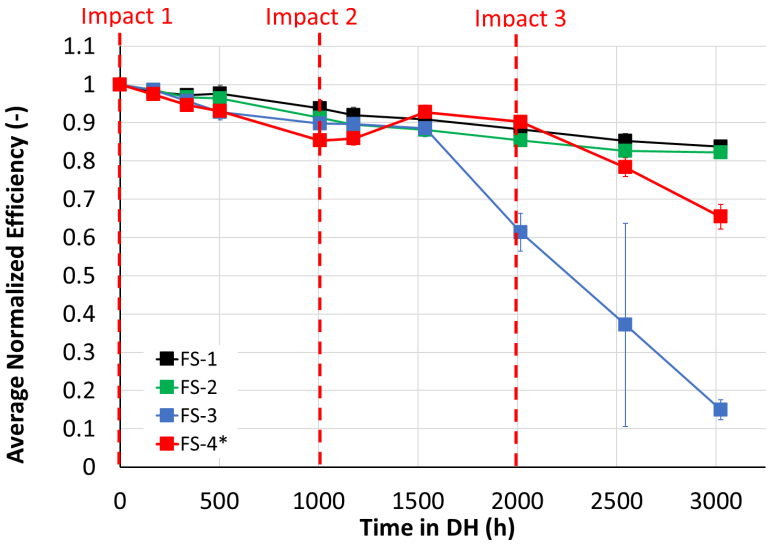

Figure 22 Average Normalized Efficiency as function of time in DH for devices with four different FSs. Each data point in the graphs represents the average taken over 5 samples. The error bars indicate the standard deviation. The red-dashed lines indicate the times at which an impact was made with the ball-drop setup. Impact 2 and Impact 3 were performed after characterization in IV, EL and PL for the 1000 h and 2000 h DH exposure, respectively.

In the combined ball-drop and DH test, FS-3 is seen to perform much worse than in only DH. After 2000 hours DH, a loss of 40% relative efficiency is observed, while in only DH 10% relative efficiency was lost after the same amount of DH exposure (see Figure 4 in section 2.1.1). The high spread observed at 2500 hours DH for FS-3 also reflects that nearly all samples had degraded to only ~10% of initial efficiency, with exception of one sample. Hence, the additional impact clearly damages the moisture protection of the devices, as also seen in PL an EL images. With approximately 90% of initial efficiency remaining after 1000 h DH, the front sheet also didn't pass the IEC criteria in this test.

FS-4* is the second worst performing front sheet in the combined ball-drop and DH test, and shows some fluctuations in performance evolution. The IEC criteria of 95% of initial efficiency after 1000 h DH is passed by FS-1 and FS-2, while FS-3 is also close to this criteria.

An additional test was performed to investigate the resilience of front sheets against scratch formation, referred to as "scratch test" in the following. As there is no IEC prescribed test for this purpose, a standardized "pencil hardness test" was used to reproducible create scratches on the SF front sheet (see Figure 23). Some results of this test for 6 different front sheets are shown in Figure 24. Distinction was made between no scratch ("G", green), indentation ("I", orange) and clear scratch ("K", red).

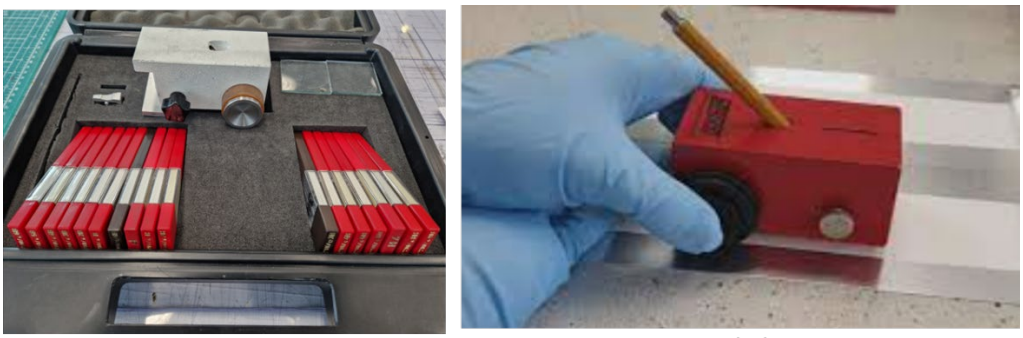

Figure 23 Pencil hardness test. (A) Test kit with 17 pencil hardnesses. (B) Illustration of the test procedure according to ASTM D3363 [6] (standard test method for hardness by pencil test).

	Damp heat time	6B	5B	4B	3B	2B	B	HB	F	H	2H	3H	4H	5H	6H	7H	8H	9H	Pencil hardness
FS A	0								G		G				i	i	K		
	1000								G	K	K	K			K				
	2000																		
	3000																		
FS B	0	K							K		K								
	1000	K							K						K		K		
	2000																		
	3000																		
FS C	0								G		G				G	i	i	i	
	1000								G			G	i		i		i		
	2000																		
	3000																		
FS D + layer 1	0								G		G				i	i	K		
	1000								G	i	i	i			i		i		
	2000																		
	3000																		
FS D	0	K							K		K								
	1000	K							K						K		K		
	2000																		
	3000																		
FS D + layer 2	0								G		G				G	G	K		
	1000								G						G	K	K		
	2000																		
	3000																		
FS E	0						G	i	i		i	K	K		K		K		
	1000								G	i		i			K		K		
	2000																		
	3000																		

Figure 24 Results of pencil hardness test for all 17 hardnesses, tested on 6 different FSs or FS configurations. Green “G” marking indicates no visible scratches. Orange “I” marking indicates indent can be felt but is not visible. Red “K” marking indicates clear scratching on the FS (complete failure).

As clear from the results of the pencil hardness test shown above, there is large variation between the scratch resistance of different front sheets. The amount of scratch resistance also clearly varies with DH exposure. This indicates for SFs with certain choice of front sheets, protection against scratching will be very important during transport and storage.

2.3.2 Protection films for storage and handling of semi-fabricates

This section focuses on finding suitable protection films for storage and transportation of SFs. These films/protection products should be designed to protect flat components during transport/storage. Furthermore, they need to protect SFs against external contamination, moisture as well as mechanical stresses. A pre-selection for suitable protection films has already been carried out. Here, various polymeric film types were assessed on their material properties and the type of adhesion they employ. With the first requirement profile, low-density polyethylene (LDPE) film was selected. This option provides a low-cost

solution with good flexibility, high impact strength, and resistance to many chemicals. Nevertheless, LDPE has certain limitations, including lower temperature resistance, increased permeability to gases, and sensitivity to contaminants. For the method of adhesion of the polymeric film, static cling as opposed to pressure sensitive adhesives was chosen. The advantage of static clings films is that they do not require any solvents, since no residues will be left after pulling off the film.

A structured survey was developed and sent out to the company partners (Schweizer, iWin and G2P). In cooperation, a refined requirement profile was then developed. Depending on the SF, the storage time is estimated to be from 3 months to about 2 years. In general, the storage time has an influence on the long-term properties of the polymeric films, although storage times of around 2 years should not be a problem for this case. The water vapor transmission rate as well as the O_2 permeability should be as low as reasonably possible. For polymers, typically the water vapor transmission rate ranges from 0.002-400 g/(m² 24h), while O_2 permeability ranges from 0.02-30000 cm³/(m² 24h). Since the products are transported in designated transport boxes, the protection of the polymeric film against external mechanical loads is not of the highest priority. Nevertheless, the polymeric film should still withstand medium impacts without immediate cracking or scratching. Impact resistance of polymers ranges from 1-700 kJ/m² at 23 °C. Expected temperatures during storage and transport of semi-fabricates are estimated to be around -10 to 50 °C. This is important information to avoid that the polymer gets too brittle or soft during its application. An extensive amount of UV load is not expected either. This is important since polymers tend to undergo chain scission under UV load if not stabilized, resulting in a change of their mechanical properties.

Figure 25 displays water vapor transmission rate vs O_2 permeability of different polymers with a price <5 €/kg and an impact strength of >20 kJ/m² at 23 °C. The price limit was set to 5 €/kg to exclude expensive polymers, since ideally the polymeric protection film should be as inexpensive as possible. For the impact strength, 20 kJ/m² at 23 °C as a minimum value is a starting point and will be refined later. With these limits applied, the water vapor transmission rate of suitable polymers (excluding Ethylene Butyl Acrylate or EBA) ranges from 0.1 to 10 g/(m² 24h). Polymers with non-polar units like LDPE, high density polyethylene (HDPE) or polypropylene (PP) as well as cellulose based polymers (CA, CN) hereby show the lowest values. Thermoplastic elastomers (TPO) show a low water vapor transmission rate, but a rather high O_2 permeability. Polyamide (PA) shows the lowest O_2 permeability amongst the remaining polymers. All the aforementioned polymers would be suitable candidates. Depending on the importance of the specific properties, one specific polymer type is superior than the other. For instance, if a higher impact strength is needed, Polyethylene (PE) well as PP are good candidates. In order to narrow the selection down further, another refinement of the properties and ranking should and will be carried out.

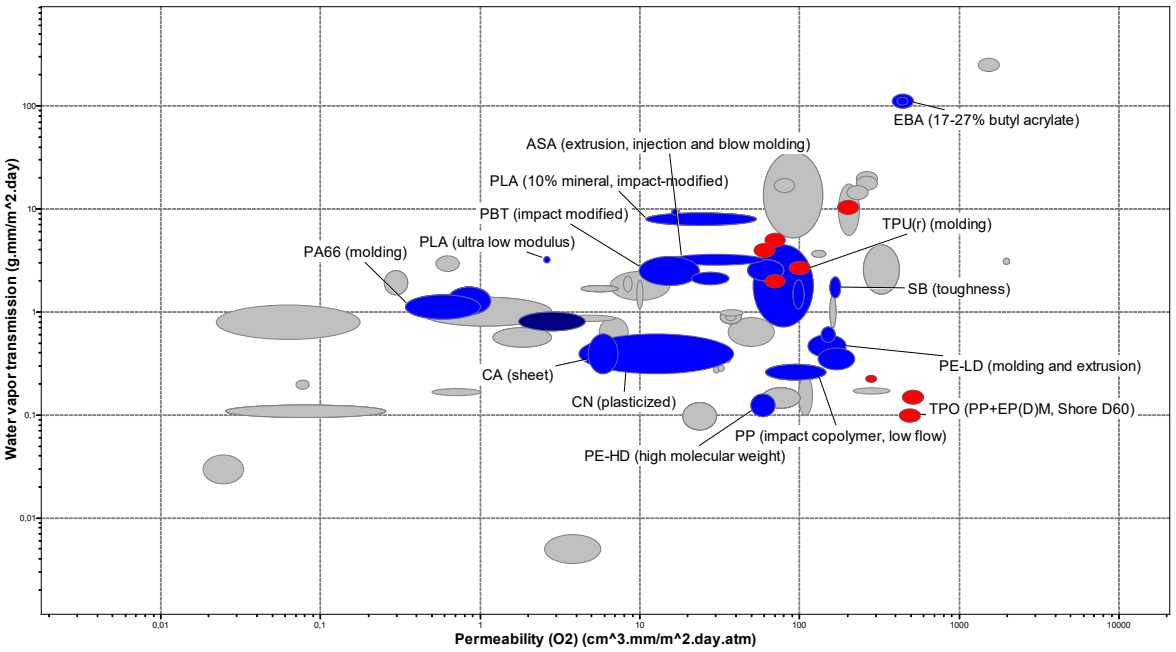

Figure 25 Water vapor transmission rate vs O_2 permeability of polymers with a price <5 €/kg and an impact strength of >20 kJ/m² @23 °C from Cambridge Engineering Selector.

3 Reliability testing of SFs for transparent BIPV back-end products

Within the framework of SF testing activities, particular care was dedicated to the innovative Heli-ON™ product technology provided by G2P. The Heli-ON™ product is basically a conventional Insulating Glass Unit (IGU) endowed with a photovoltaic technology for electrical power generation. Such an end-product and related SF components have been already reported and fully described in deliverable D2.9 and are highlighted in Table 6 of this document. The activities reported in the following are aimed at providing both technical and economical insights into different commercially available c-Si PV module technologies. A testing scheme was defined to determine the performance and reliability of different SFs already on the market which were of interest for integration into the PV IGU archetype. This was performed in parallel with task 2.7 (Reliability testing of IPV end products).

3.1.1 Reliability testing feedback towards optimization of manufacturing process parameters

The reliability testing was performed to provide feedback to the product owners with a focus towards optimization of manufacturing process parameters. Testing campaigns performed for the Heli-ON™ end-product are reported in Table 6. Moreover, SF reliability tests are highlighted in orange.

Phase 1 focused on prototypal product reliability tests, and related results have been exploited to trigger further assessment of different market suppliers and their c-Si mini-modules. Therefore, during Phase 2, 10 PV arrays (i.e., a sample made by 3 identical SF connected in parallel) underwent 100 thermal cycles, with a mid-characterization after 50 cycles. Hence, 30 SFs were tested to provide an overview on the performance and reliability after accelerated ageing. The results obtained were then considered for successive optimization and investigation of the updated end-product design (Phase 3). An additional 18 PV arrays to provide further insights into the reliability of different c-Si SF suppliers.

Table 6 Overview of reliability testing design of experiments for PV IGU archetype

Product	Test Phase	Test Description	Samples
A	**Phase 1: Initial End Product Testing**	100 x Thermal Cycles	**1** x IGU, **1** x PV frame **2** x PV Array (each with 6 rows of 10 in parallel-semifabricates)
		Characterization → 100 TC → Characterization	
	Phase 2: Semifabricates Testing	100 x Thermal Cycles Tests	**10** x PV array (each with 3 in parallel-semifabricates)
		Characterization → 50 TC → Characterization → 50 TC → Characterization	
B	**Phase 3: Updated End Product Testing**	100 x Thermal Cycles + 10 x Humidity Freeze	**2** x IGU, **1** x PV frame **18** x PV Array (each with 3 in parallel-semifabricates)
		Characterization → 50 (30) TC → Characterization → 50 (70) TC → Characterization → 10 HF → Characterization	
		500 h Damp Heat Tests	**2** x IGU
		Characterization → 500 h DH → Characterization	
	Phase 4: Semifabricates Handling & Storage Testing	Electroluminescence & I-V Curves Characterization	**6** x SF Types (totalling **342** SF samples)
		Characterization	

Legend *IGU: Insulated Glass Unit TC: Thermal Cycles HF: Humidity Freeze DH: Damp Heat*

The definitions of the different tests indicated are summarized as follows:

Thermal cycles (TC) in cycles:

Temperature cycles between -40 °C and 85 °C following times given by IEC61215 [2]

(total time of 3-6 hours, typically 100 or 200 cycles)

No current injection

3 h per cycle

Total time: 9000 minutes = 150 h = 50 cycles with maximum temperature (T_{MAX}) = 85 °C, minimum temperature (T_{MIN}) = -40 °C

Damp heat (DH) in hours (h):

85 °C and 85 % relative humidity (RH) (typically for 500, 1000 or 2000 h)

Humidity Freeze (HF) in cycles:

85 °C and 85 % RH for 20h -> cycle to -40 °C (typically 10 cycles)

Compared to typical test: No current injection

Characterization:

I-V curve (performance measurement using A+A+A+ flash tester)

Visual image.

EL image

The definition of the samples within these archetype tests are as follows:

Semi-fabricates:

- PV semi-fabricates: fully laminated c-Si based PERCMONO or IBC technology with average nominal Maximum Power Point (P_{MAX}) = 3,10 W; Maximum Power Point Current (I_{MPP}) = 0,20 A; Maximum Power Point Voltage (V_{MPP}) = 15,50 V for samples tested in Phase 2; P_{MAX} = 2,81 W; I_{MPP} = 0,19 A; V_{MPP} = 15,66 V for samples tested in Phase 3.
- PV array: device made by 3 PV SFs connected electrically in parallel and physically linked by aluminium bars)
- PV frame: a metallic supporting frame with a certain number of PV SFs around its entire perimeter.

End Products:

- Photovoltaic Insulating glass unit (PV IGU): Prototype of PV window, made by the PV frame integrated within two glass panes.

As shown in Table 7, during Phase 3 for each of the 18 PV arrays tested, electroluminescence measurements were performed as well as three I-V curves (measurements are included in Appendix A). The changes under thermal cycles were reported and a complete overview of the normalized power drop of all samples tested is presented in Figure 26, together with results from Phase 2. Note the second testing campaign had intermediate measurements at 30 TC prior to 100 TC due to a malfunction of the climatic chamber during the testing campaign.

These results highlighted the difference between manufacturers and the production, handling, and storage of these semi-fabricates. From here further testing (Phase 4) of SF was performed with an emphasis on handling and storage of the semi-fabricates being sent from the manufacturers, with the aim to gain insights on the causes of damage of PV cells and in turn provide feedback into improved practices for handling and storage to the product owner and suppliers of these semi-fabricates.

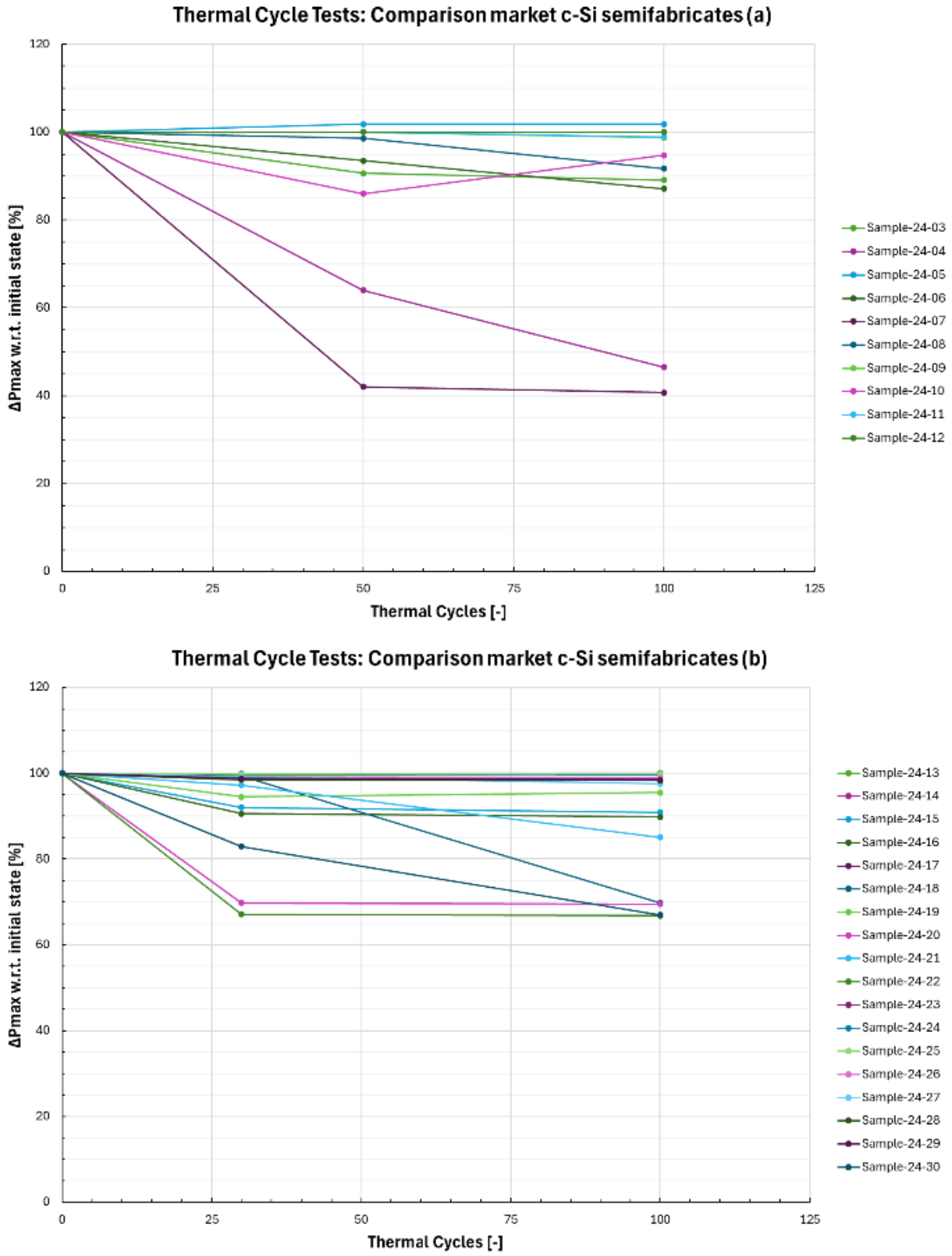

Figure 26 TC test results within reliability testing of transparent back-end products . a) Initial market batch sample tested in Phase 2 and b) second market batch sample tested in Phase 3 for a total of 100 cycles (150 hours of testing for each sample)

Table 7 EL and I-V curves examples of different SF samples tested for 100 TC and their respective normalized maximum power drop under STC. Samples refer to Sample ID 24-06 (top), to Sample ID 24-03 (middle) and to Sample ID 24-08 (bottom) investigated during Phase 2.

	0 thermal cycles	50 thermal cycles	100 thermal cycles
IV	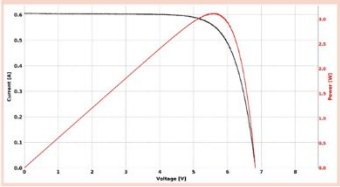	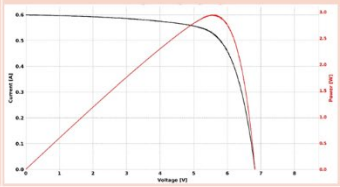	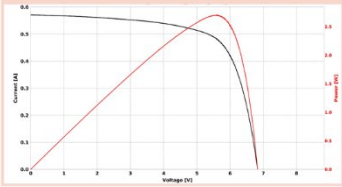
ΔP_m	-	- 6.5 %	- 12.9 %
EL	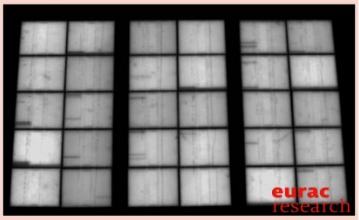	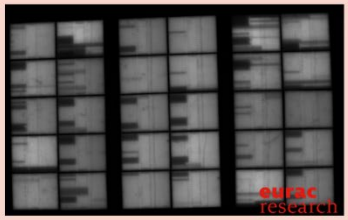	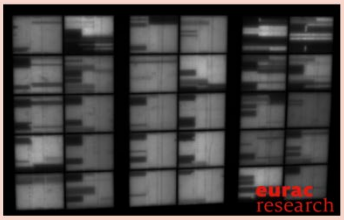

	0 thermal cycles	50 thermal cycles	100 thermal cycles
IV	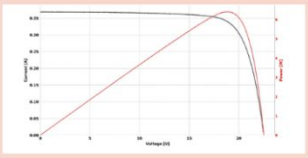	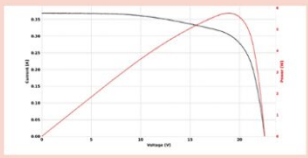	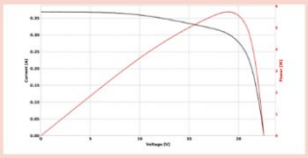
ΔP_m	-	- 9.4 %	- 10.9 %
EL	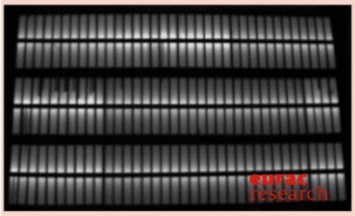	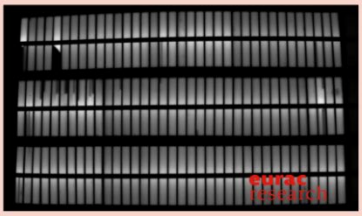	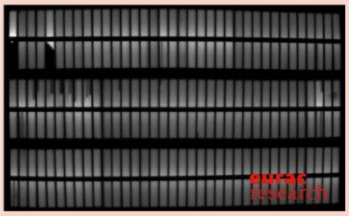

	0 thermal cycles	50 thermal cycles	100 thermal cycles
IV	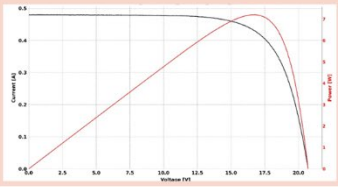	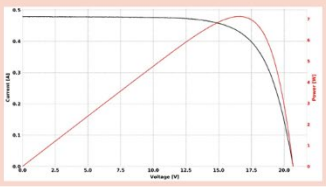	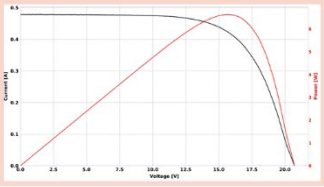
ΔP_m	-	- 1.4 %	- 8.3 %
EL	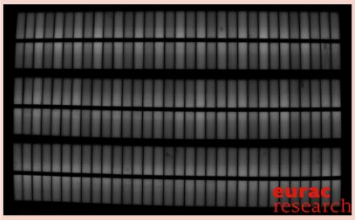	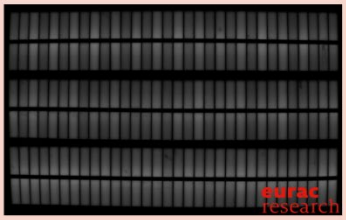	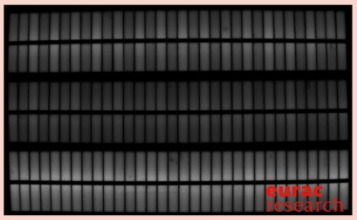

3.1.2 Handling, storage and transport of SF effects on reliability

Phases 2 and 3 were also used for further study the reliability of the potential SF to be used in this archetype. Power, voltage, and current at MPP were measured with a maximum 2.9% uncertainty and were plotted against nominal values provided by manufacturers. The error bars representing measurement uncertainty and manufacturing tolerance (±5% for nominal, ±2.9% for measured) suggest that while most modules fall within expected variability, several samples approach or exceed the lower uncertainty bounds, raising potential concerns about consistency in manufacturing or early performance degradation.

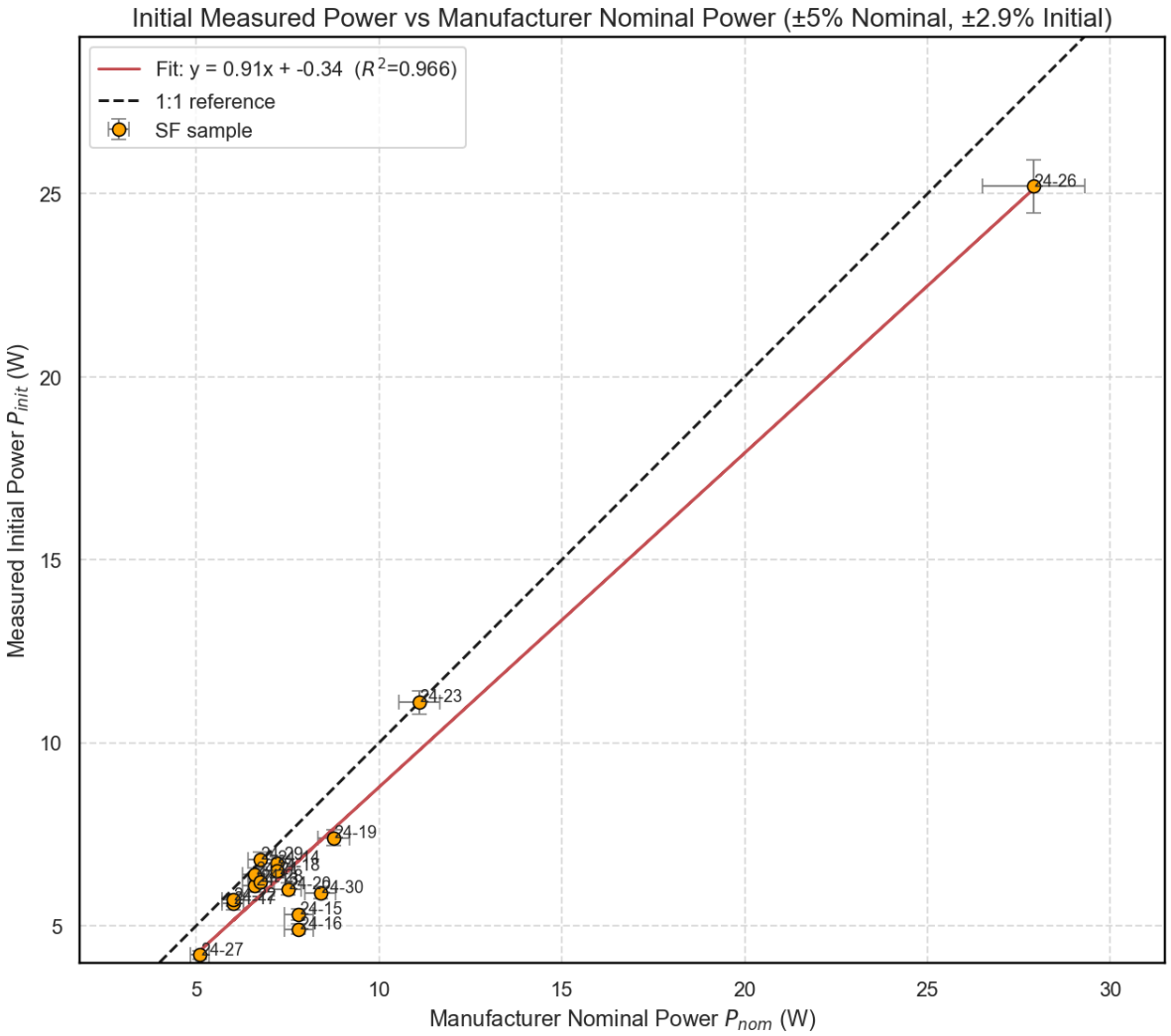

Figure 27 Measured Pmpp values measured at STC (with +-2.9% uncertainty) for tests performed against manufacturers claimed values (including +- 5% deviation)

Thus, after Phases 2 and 3 were completed, further assessments on the final SF were performed to ensure the reliability of SF from the market at large scale (phase 4). For this reason, 137 samples divided into two were ordered and the handling and storage of the received products from the manufacturers was recorded and reported together with the EL and IV tests performed. For details, see Table 8 to Table 10.

Table 8 Semi-fabricates samples tested with respect to handling and storage

Sample Label	IV curves performed	EL images performed	Total sample number
AE (A-ETFE)	60	100	100
AP (A-PET)	20	20	20
BE (B-ETFE)	10	40	100
BP (B-PET)	10	15	15
CE (C-ETFE)	20	31	100
CP (C-PET)	17	17	17

Table 9 Handling and storage of SFs as received from manufacturers

Handling type	Visual Image		Handling and Storage Description
	Batch	Semi-fabricate	
I AE & AP Samples	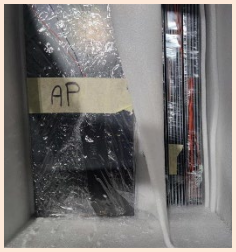		**Shipping external protection:** Carton box **Internal protection:** Perimeter foam protection Horizontal & vertical stacking with plastic protector between large sets of SF (5-10)
II BE & BP Samples			**Shipping external protection:** Carton box **Internal protection:** Vertical stacking with plastic bubble wrap protector between large sets of SF (5) and internal plastic protector between individual SF front side (1)
III CE & CP Samples		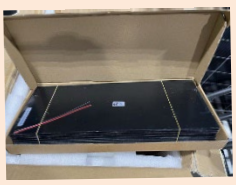	**Shipping external protection:** Carton box **Internal protection:** Perimeter foam protection Horizontal stacking with carton box protection between large sets of SF (5-10)

Table 10 Electroluminescence test samples overview of the second samples (example) taken for each of the supplied SF types

Handling type	Visual Image	
	ETFE	PET
I AE & AP Samples	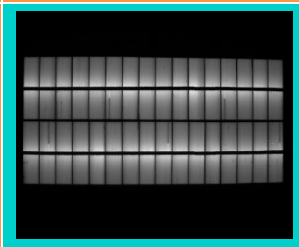 Sample: AE-02	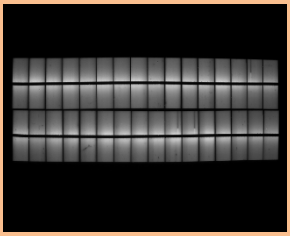 Sample: AP-02
	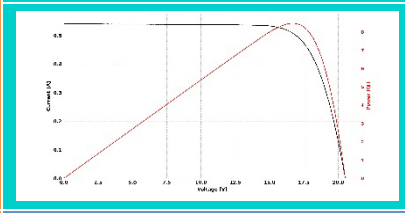	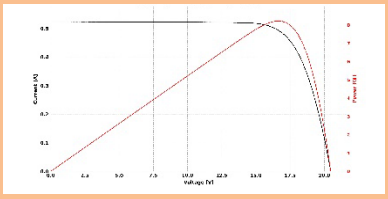
II BE & BP Samples	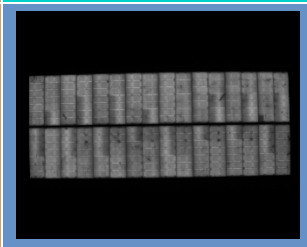 Sample: BE-02	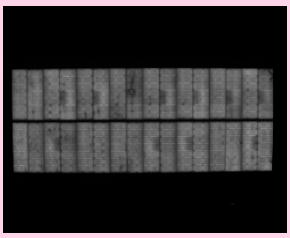 Sample: BP-02
	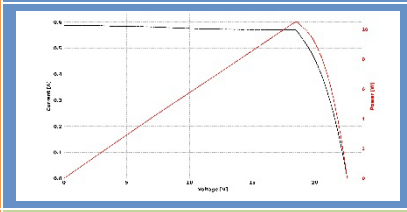	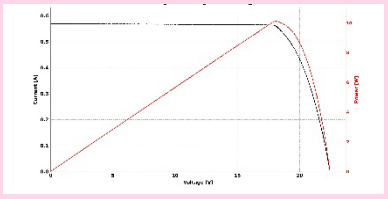
III CE & CP Samples	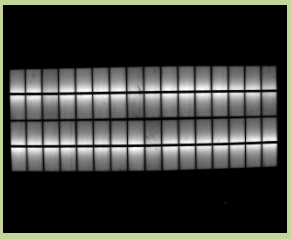 Sample: CE-02	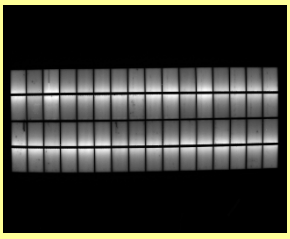 Sample: CP-02
	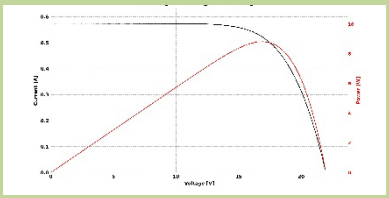	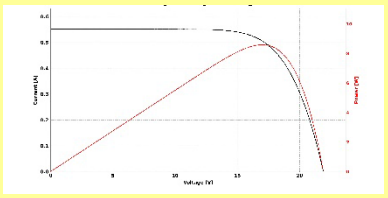

The I-V test results are presented in Figure 28. The boxplots zoom out (plot with axis starting at 0), show one additional CP sample which had a 0 A measurement, and is thus included in Appendix C for completeness of measurements.

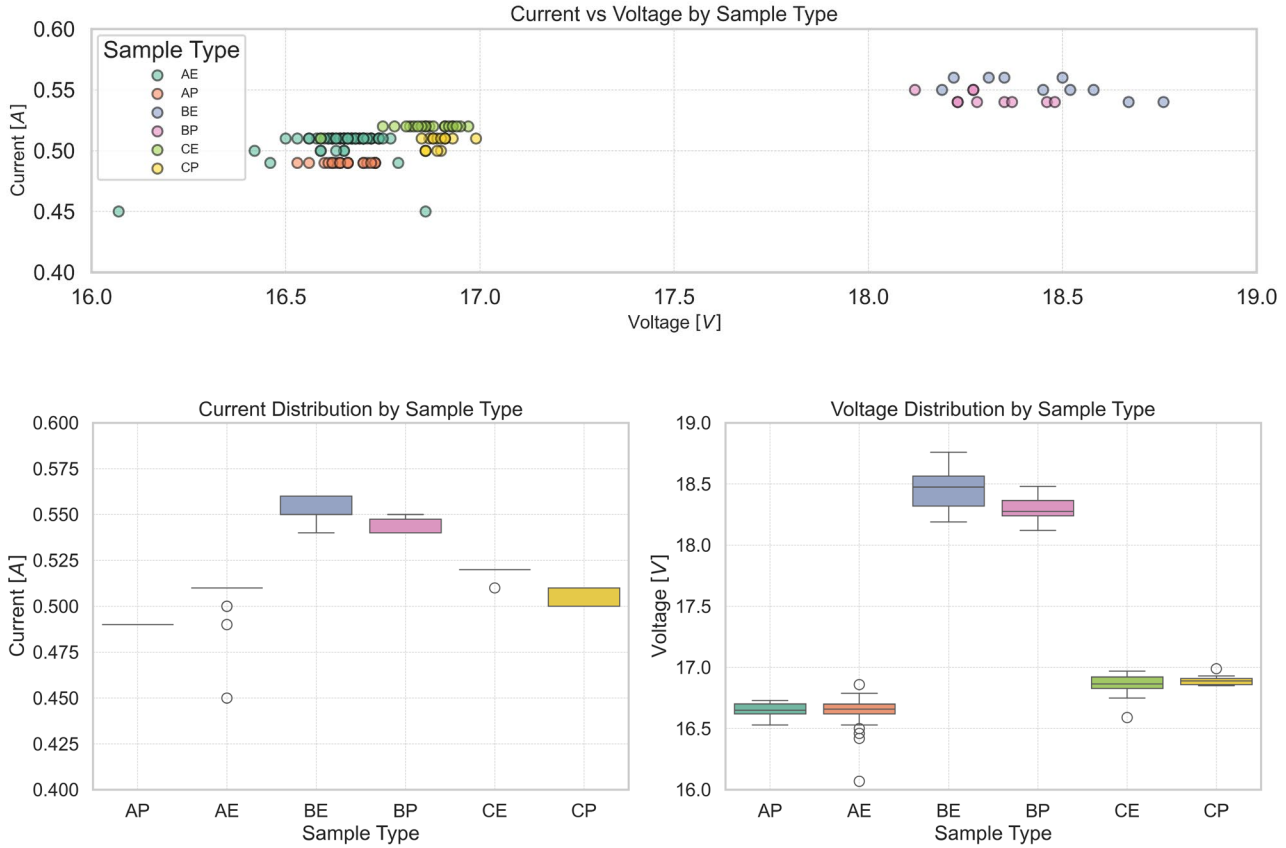

Figure 28 I-V test results classified by handling type with current (Impp) and voltage (Vmpp) boxplot distributions per sample type

An analysis of maximum power point (MPP) voltage (V_{MPP}) and maximum power point current (I_{MPP}) across SF types tested shows clear differences in performance. AP and CE show consistent current (at MPP) measurements, while for voltage (at MPP) AP, AE, CE and CP show the most consistent results when analysing the boxplots. The changes in Impp within a single SF technology indicate a possible reduction of the active area due to cracks in the cells. V_{MPP} usually changes less but may be affected by series resistance.

AP and CE modules deliver the best balance of voltage and current, with power output consistent throughout samples. BE and BP modules operate at higher voltages (>18 V) and currents (>0.53), so a higher output but with greater variability. AE and CP samples show a higher variability in voltage and current when compared to samples AP and CE, indicating a reduced consistency in power output. The spread in data, especially in lower-performing sample batches, likely reflects variability between samples, often caused by microscopic defects, contact issues, or material inconsistencies seen in EL tests. These factors can lower the current by disrupting carrier flow or reducing voltage through increased series resistance. The highest power outputs were seen for samples BE and BP, which also had the most protection, concerning handling type II of protection (shipping internal and external protection) as described within Table 8 to Table 10. Further analysis should be made by performing additional I-V and EL tests by manufacturers before sending the sample to identify the extent to which performance may be affected by transport, handling, and storage and thus provide guidelines to the manufacturer for improved handling of the SF procedure.

Conclusions

Reliability tests on generic SFs for integration into BIPV helped significantly narrow down the potential BoM, and allowed optimization of processing to reach highly reliable SFs form the MC-line. The DH tests on front sheets showed more than one candidate for good moisture protection. The current choice was mainly made based on material availability at the time. However, research into alternative front sheets with collaboration of front sheet suppliers is still ongoing. This can help identify cheaper, more flexible and possibly ETFE-free front sheets for future use. Tests on the back sheet showed a thinner material than conventionally used for S2S lamination was beneficial for SF lifetime, especially in R2R lamination. This choice of back sheet also seems to allow incorporation of Cu-cladding directly into the back sheet, and Cu-milling without compromise to the moisture protection. Initial tests on PO encapsulants in R2R lamination showed the main challenge to be the TC test, where none of 6 PO's allowed sufficient reliability. Of the three best performing PO-3, PO-4 and PO-5, PO-3 was found to give the best combination of reliability and processibility. However, additional optimizations on PO-1 and PO-5 also showed the potential for better performance in other PO's with more detailed fine-tuning. Hence, research on suitable POs is still ongoing achieve a better R2R process and reliable SF.

Just as for PO, the biggest challenge for ECAs was found in the TC testing of devices. Tests on CIGS devices showed best results for a lower silver content ECA. While this would be promising for increasing sustainability of the SFs and reducing ECA costs, at the moment a conventional ECA is still used while the positive results for low silver are being validated. Edge sealant ES-2, based on butyl rubber of 0.6 mm thick was found to be suitable for passing the 1000 h DH test in R2R laminated devices.

From comparison of lamination speeds and pressure, it was found that R2R lamination at 0.3 m/min with high pressure from the rolls gave the most stable results. SFs produced with this approach passed the DH test quite easily. Tests on TC and HF were still ongoing at the time of writing.

Testing the sensitivity of front sheets to impact and scratching showed a large spread between different front sheets. This highlighted the importance of adding protective foil to SFs for transport and storage. A first assessment of suitable materials for a protective film of generic SFs showed that LDPE would be a cost-effective choice, although PE and PP were also found as good candidates depending on precise requirements.

The reliability testing of SFs for transparent BIPV back-end (specifically IGUs) revealed significant performance differences among commercial c-Si SFs for these applications. Variability was linked to manufacturing quality, PV cell quality, and handling and storage conditions during transport. TC, DH, and EL/I-V test campaigns showed that certain SF types provided stable performance, while others exhibited degradation due to presence of micro-cracks or inconsistent quality. These findings support the need for reliable testing from manufacturing (from accredited tests), standardized handling protocols, and pre-shipment testing to improve the reliability and performance of PV SF to ensure a constant quality and reliability prior to their integration within end-products.

References

[1] International Electrical Commission, *IEC61215-1-2021, Terrestrial photovoltaic (PV) modules - Design qualification and type approval - Part 1: Test requirements,* International Electrical Comission, 2021.

[2] International Electrical Commission, *IEC61215-2-2021, Terrestrial photovoltaic (PV) modules - Design qualification and type approval - Part 2: Test procedures,* International Electrical Comission, 2021.

[3] International Electrical Commission, *IEC61730-2-2023, Photovoltaic (PV) module safety qualification - Part 1: Requirements for testing,* 2021.

[4] S. V. e. al., "Insights into the moisture-induced degradation mechanisms on field-deployed CIGS modules," *Progress in Photovoltaics,* p. 15, 2022.

[5] "European Chemicals Agency (ECHA)," ECHA, 15th July 2021. [Online]. Available: https://echa.europa.eu/registry-of-restriction-intentions/-/dislist/details/0b0236e18663449b. [Accessed 06 June 2025].

[6] *ASTM D3363-22,* ASTM International, 2022.

Appendix A

In this appendix the results of material properties tests on PO encapsulants are reported, that allowed selection of the most promising POs for reliability testing and use in the MC line. The aim of this research was to evaluate different encapsulants on their applicability for roll-to-roll lamination and finding the optimal process window for the use of these encapsulants on the mass customization line. Therefore, at PCCL, the encapsulants were tested according to polymer scientific standards with DSC (Differential scanning Calorimetry), DMTA (Dynamic Mechanical Thermal analysis), FTIR (Fourier-transform infrared spectroscopy), DIC (Digital Image Correlation) and on a heating plate.

Table 11 Results from tested encapsulants with DSC, DMTA, FTIR and on a hot plate.

Sample		DSC				DMTA		
	Origin	Tm Peak [°C]	Tx Peak [°C]	Tx Onset [°C]	material	Tsoft [°C]	Tm [°C]	Hot plate
PO1	TNO	92			Ethylene ethyl acrylate copolymer	71	97	
PO2	TNO	75	166	144	Ethylene α-olefin copolymer	74	93	warps
PO3	TNO	74			Ethylene based coploymer	75	93	warps
PO4	TNO	72			Ethylene based coploymer	66	93	warps
PO5	TNO	60	157	148	Ethylene α-olefin copolymer	60	78	
PO6	TNO	91			Ethylene ethyl acrylate copolymer	72	93	
PO7	PCCL	73			Ethylene α-olefin copolymer	71	110	
PO8	PCCL	103			Ethylene α-olefin copolymer	67	101	
PO9	PCCL	121			Ethylene α-olefin copolymer	54	76	

Table 11 shows the combined results from all tested encapsulants. The requirements on the material for roll to roll encapsulation are:

a) Low melting temperature
b) Early onset of crosslinking temperature or no crosslinking during lamination
c) low softening and melting temperature
d) Low anisotropy

Regarding the material properties form table 1, PO3 and PO4 seem to be most suitable candidates for roll-lamination. Work on the mass customisation line showed PO5 to be the most promising material, but it is still open to what degree the material is crosslinked after lamination.

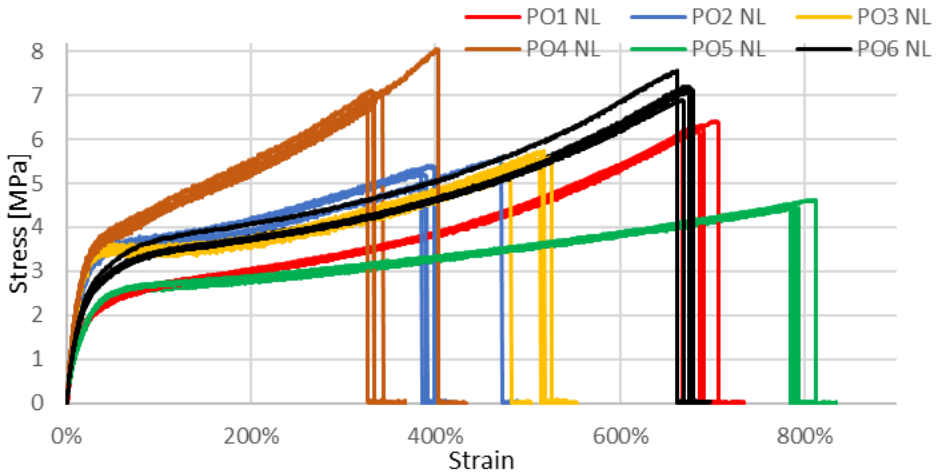

Figure 29 Stress-strain graph of non-laminated POs.

Analysis of the tensile strength of the POs, measured until breakage, shows that there are large differences in stress resistance and amount of strain (visible in Figure 29). The breaking-point stresses are ranging from 4 to 8MPa while strain percentages are ranging from 350 to 800%.

Table 12 Results of creep testing.

Enc.	Creep	Dewetting	Size	Amount
PO1	N	N	N.a.	N.a.
PO2	N	Y	1	5
PO3	N	Y	2	4
PO4	N	Y	3	3
PO5	Y	Y	5	1
PO6	N	N	N.a.	N.a.

Creep testing was executed, with the results shown in Table 12. The presence of creep, which is the displacement of the pieces of front sheet in relation to each other, and dewetting are shown. For dewetting, the size and amount of defects is ranked on a scale compared to each other from 1 to 5, with 1 being the smallest or lowest amount, and 5 being the biggest or highest amount.

Appendix B

This appendix contains the results of material tests performed on ES for the purpose of defining the best processing approaches. Dynamic Mechanical Thermal Analysis (DMTA), thermogravimetric analysis (TGA) and differential scanning calorimetry (DSC) analysis were performed. Peel testing was used to assess the strength of the adhesion of the sealant in the laminate were R2R processing was compared to S2S.

The results were used to select materials and processing settings for the reliability tests for which results are reported in section 2.1.6. Three ESs were evaluated, the properties of each ES are summarized in in Table 13.

Table 13: Type and properties of the used edge sealants.

	ES1	ES2	ES3
Thickness	0.4mm; 0.6mm	0.615mm	0.05mm
Main material	Butyl rubber	Butyl rubber	Undisclosed
Main fillers	Molecular sieve desiccant	Molecular sieve desiccant	Molecular sieve desiccant
Form	Tape (roll)	Tape (roll)	Sheets
Colour	Black	Black	Beige

TGA showed that ES3 has an important weight loss in the temperature range corresponding to lamination DH conditions (80-150°C). ES1 and ES2 were much more stable in this temperature range and showed little weight loss. The weight loss is attributed to the release of water from the molecular sieve getter. DSC measurements on the materials did not show phase changes in the temperature range 80-150°C. However, differences between the first and second run of DSC indicated that indeed water is being lost from the material upon heating. Laminated (i.e. heat treated) material did not show this effect indicating processing also helps to release any present water in the edge sealants. Since ES3 was extremely thin, the DMTA could only be performed on ES2 and ES1 (See Figure 30). This showed ES1 was more flexible and elastic than ES2 at room temperature. The complex shear modulus of ES2 is significantly lower in the temperature range used for roll lamination. This also explains why it is easier to laminate air enclosures out of ES2 than ES1, resulting in a better and more stable edge seal.

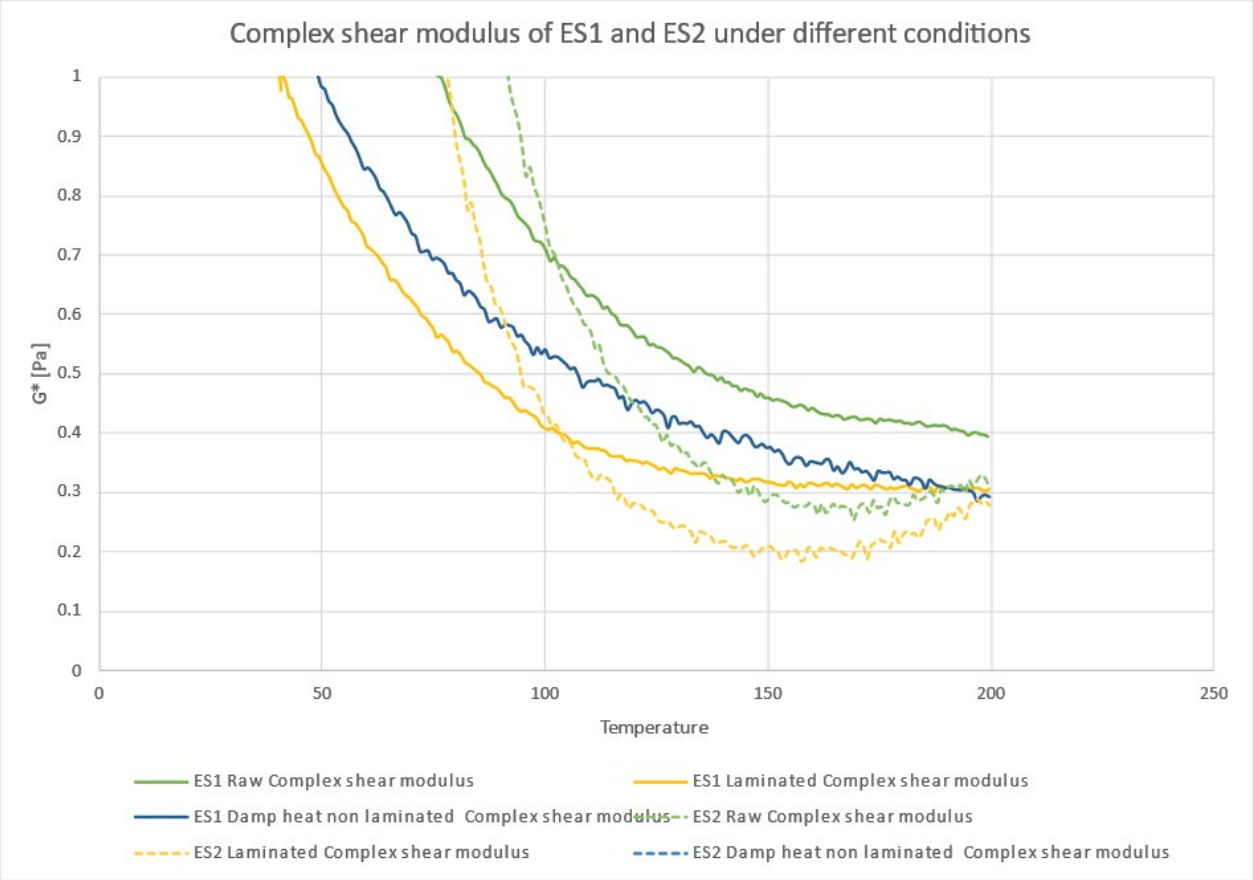

Figure 30: Viscoelastic behaviour of the two butyl rubber based edge seals.

Appendix C

This appendix provides the I-V measurements performed under STC for SF during the TC testing campaign of G2P partner. Experimental outcomes from Phase 2 are reported in Table 6, while those from Phase 3 are reported in Tables 7-8.

Table 14 SF samples (PV window frame) measurements during Phase 2 (10 samples)

Sample	Thermal cycles	T_{dut} / °C	Irr / W/m²	I_{sc} / A	V_{oc} / V	P_{max} / W	Fill factor / %	I_{mpp} / A	V_{mpp} / V	P_{max} corrected / W	ΔP_{max} w.r.t. initial state / %
24-03	Nominal Value	-	-	-	18.00	-	-	-	-	-	-
	0	25.1	1000.4	0.37	22.61	6.4	76.9	0.34	18.83	6.40	
	50	24.9	999.8	0.37	22.66	5.8	68.8	0.3	18.91	5.80	**-9.4**
	100	24.7	1000.2	0.37	22.68	5.7	68.5	0.3	18.95	5.70	**-10.9**
24-04	Nominal Value	-	-	0.50	25.20	9.30	-	0.47	19.80	-	-
	0	25.1	1000.4	0.47	24.37	8.6	75.3	0.43	19.88	8.62	
	50	24.7	999.8	0.31	24.66	5.5	71.4	0.28	19.88	5.51	**-36.0**
	100	25.1	1000	0.31	26.71	4	48.1	0.26	15.45	4.01	**-53.5**
24-05	Nominal Value	-	-	-	13.00	-	-	-	-	-	-
	0	25.3	1000.3	0.44	16.31	5.6	78.9	0.41	13.69	5.60	
	50	25.2	999.9	0.44	16.31	5.7	78.9	0.41	13.69	5.70	**1.8**
	100	25.1	1000	0.44	16.33	5.7	78.8	0.41	13.71	5.70	**1.8**
24-06	Nominal Value	-	-	0.67	6.30	3.00	-	0.60	5.00	-	-
	0	25.2	1000.6	1.36	6.83	3.1	33.5	0.56	5.58	3.12	
	50	25.1	1000	1.32	6.83	2.9	32.5	0.53	5.57	2.92	**-6.5**
	100	24.7	1000.3	1.24	6.84	2.7	31.8	0.49	5.56	2.71	**-12.9**
24-07	Nominal Value	-	-	-	17.00	9.00	-	-	-	-	-
	0	25	1000.4	0.5	21.83	8.1	74.7	0.45	17.91	8.12	
	50	25.2	999.7	0.23	29.13	3.4	49.5	0.19	18.25	3.41	**-58.0**
	100	25.3	1000	0.23	32.89	3.3	43.8	0.19	17.87	3.31	**-59.3**
24-08	Nominal Value	-	-	-	17.00	9.00	-	-	-	-	-
	0	25.2	1000.3	0.48	20.76	7.2	72.3	0.43	16.69	7.20	
	50	25.4	999.8	0.48	20.74	7.1	71.8	0.43	16.57	7.10	**-1.4**
	100	25.1	1000	0.48	20.67	6.6	67	0.42	15.67	6.60	**-8.3**

24-09	Nominal Value	-	-	0.60	-	10.50	-	0.56	18.56	-	-
	0	25.2	1000.4	0.52	21.56	7.7	69	0.43	18	7.72	
	50	25.1	999.8	0.52	21.56	7.7	69.2	0.43	17.73	7.72	**0.0**
	100	24.9	1000.1	0.52	21.58	7.6	68.5	0.43	17.9	7.62	**-1.3**
24-10	Nominal Value	-	-	0.60	-	10.50	-	0.56	18.56	-	-
	0	25.2	1000.3	0.5	21.76	5.7	52.2	0.32	18.07	5.63	
	50	25.2	999.7	0.5	22.38	4.9	43.8	0.35	13.95	4.84	**-14.0**
	100	24.8	1000.1	0.5	21.79	5.4	49.5	0.28	19.64	5.33	**-5.3**
24-11	Nominal Value	-	-	-	17.00	9.45	-	0.65	14.50	-	-
	0	25.1	1000.4	0.74	16.38	8.8	72.4	0.63	13.86	8.86	
	50	25.1	999.9	0.74	16.39	8.8	72.6	0.63	13.89	8.86	**0.0**
	100	25	1000	0.74	16.39	8.7	72.4	0.63	13.91	8.76	**-1.1**
24-12	Nominal Value	-	-	-	17.00	9.45	-	0.65	14.50	-	-
	0	25.2	1000.4	0.73	16.32	8.6	72.5	0.63	13.79	8.66	
	50	25	999.8	0.73	16.32	8.6	72.2	0.63	13.79	8.66	**0.0**
	100	24.8	1000.1	0.73	16.34	8.6	72.2	0.62	13.8	8.66	**0.0**

Table 15 SF samples (PV window frame) measurements during Phase 3 (18 samples – Part One)

Sample	Thermal Cycles	Tdut / °C	Irr / W/m2	Isc / A	Voc / V	Pmax / W	Fill factor / %	Impp / A	Vmpp / V	Pmax corrected / W	Pmax RAW / W	ΔPmax RAW w.r.t. initial state / %
24-13	Nominal Value	-	-	-	-	6.60	-	0.45	16.50	-	-	-
	Initial	25.3	999.9	0.42	18.82	6.1	76.2	0.39	15.51	6.10	6.07	
	TC30	25.4	1000.5	0.42	18.81	6	76.2	0.39	15.49	6.00	6.05	-0.4
	TC100	24.9	1000.5	0.42	18.87	6.1	76.3	0.39	15.57	6.10	6.07	0.0
24-14	Nominal Value	-	-	0.53	16.50	7.20	-	0.48	15.00	-	-	-
	Initial	25.2	999.9	0.44	20.11	6.7	75.3	0.41	16.25	6.70	6.70	
	TC30	25.6	1000.4	0.44	20.12	6.6	74.9	0.41	16.2	6.60	6.62	-1.1
	TC100	24.8	1000.3	0.44	20.16	6.6	74.6	0.41	16.19	6.60	6.62	-1.2
24-15	Nominal Value	-	-	-	-	7.80	-	0.45	17.50	-	-	-
	Initial	25	1001	0.38	21.08	5.3	65.8	0.32	16.25	5.30	5.26	
	TC30	25.1	1000.4	0.36	20.97	4.8	64.1	0.28	17	4.80	4.83	-8.0
	TC100	24.7	1000.2	0.36	21.01	4.8	63.6	0.28	16.76	4.80	4.78	-9.1
24-16	Nominal Value	-	-	-	-	7.80	-	0.45	17.50	-	-	-
	Initial	25.1	1000.1	0.38	20.91	4.9	61.5	0.31	16	4.90	4.94	
	TC30a	24.8	1000.4	0.33	20.94	4.5	65.4	0.28	15.92	4.50	4.47	-9.4
	TC100	25.1	1000.2	0.33	20.94	4.4	64.9	0.28	15.79	4.40	4.44	-10.2
24-17	Nomin Value	-	-	-	-	6.00	-	0.42	15.30	-	-	-
	Initial	25.3	1000	0.42	17.03	5.6	77.1	0.4	14.1	5.60	5.56	
	TC30	24.9	1000.3	0.42	17.05	5.6	77.5	0.39	14.1	5.60	5.55	-0.1
	TC100	24.6	1000.5	0.42	17.07	5.6	77.5	0.39	14.11	5.60	5.56	0.0
24-18	Nominal Value	-	-	0.53	16.50	7.20	-	0.48	15.00	-	-	-
	Initial	24.8	1001.2	0.43	20.1	6.5	75.1	0.4	16.26	6.50	6.55	
	TC30	24.9	1000.4	0.43	20.12	6.5	75.1	0.4	16.26	6.50	6.50	-0.7
	TC100	25.1	1000.2	0.37	20.1	4.6	61.4	0.27	17.09	4.60	4.57	-30.2
24-19	Nominal Value	-	-	0.69	15.50	8.76	-	0.62	14.00	-	-	-
	Initial	24.9	1000.1	0.63	16.33	7.4	71.7	0.54	13.67	7.40	7.43	
	TC30	24.5	1000.6	0.63	16.36	7	68.1	0.53	13.23	7.02	7.02	-5.5
	TC100	24.8	1000.5	0.63	16.37	7.1	68.8	0.53	13.3	7.12	7.09	-4.5
24-20	Nominal Value	-	-	0.52	19.50	7.50	-	0.48	16.00	-	-	-
	Initial	25.4	999.8	0.41	20.05	6	72.6	0.38	15.92	6.00	5.97	

	TC30	24.7	1000.3	0.35	20.11	4.2	59.6	0.26	16.11	4.20	4.17	-30.2
	TC100	24.9	1000.3	0.35	20.12	4.2	59.2	0.26	16.07	4.20	4.15	-30.5
24-21	Nominal Value	-	-	-	-	6.60	-	0.45	16.50	-	-	-
	Initial	24.8	999.9	0.44	18.87	6.4	77	0.41	15.61	6.40	6.39	
	TC30	24.8	1000.5	0.44	18.89	6.2	75.2	0.4	15.42	6.20	6.21	-2.8
	TC100	24.9	1000.5	0.44	18.89	5.4	65.8	0.35	15.75	5.40	5.44	-14.9
24-22	Nominal Value	-	-	-	-	6.00	-	0.42	15.30	-	-	-
	Initial	25.2	1000	0.44	17.04	5.7	76.6	0.41	14.04	5.70	5.72	
	TC30	24.9	1000.3	0.29	17.09	3.8	77.2	0.27	14.09	3.80	3.83	-32.9
	TC100	25.2	1000.4	0.29	17.07	3.8	77.3	0.27	14.07	3.80	3.82	-33.2
24-23	Nominal Value	-	-	0.97	16.32	11.10	-	0.85	12.96	-	-	-
24-23	Initial	25.2	999.7	0.88	16.32	11.1	76.7	0.82	13.45	11.10	11.09	
	TC30	25.4	1000.5	0.88	16.31	11	76.6	0.82	13.43	11.03	10.98	-0.9
	TC100	25.2	1000.5	0.88	16.33	10.9	76.1	0.81	13.4	10.93	10.93	-1.4

Table 16 SF samples (PV window frame) measurements during Phase 3 (18 samples – Part Two)

Sample	Thermal Cycles	Tdut / °C	Irr / W/m2	Isc / A	Voc / V	Pmax / W	Fill factor / %	Impp / A	Vmpp / V	Pmax corrected / W	Pmax RAW / W	ΔPmax RAW w.r.t. initial state / %
24-24	Nominal Value	-	-	-	-	7.20	-	-	17.00	-	-	-
	Initial	24.9	999.7	0.4	21.09	6.1	72.8	0.36	16.68	6.10	6.08	
	TC30	25.1	1000.5	0.39	21.09	6.1	72.9	0.36	16.69	6.10	6.07	-0.2
	TC100	25.4	1000.3	0.4	21.09	6.1	72.8	0.36	16.69	6.10	6.06	-0.3
24-25	Nominal Value	-	-	-	-	7.20	-	-	17.00	-	-	-
	Initial	24.9	999.6	0.38	21.11	5.9	73.2	0.35	16.76	5.90	5.94	
	TC30	24.9	1000.4	0.38	21.1	5.9	73.2	0.35	16.75	5.90	5.93	-0.2
	TC100	24.9	1000.5	0.38	21.11	5.9	73.2	0.35	16.76	5.90	5.94	-0.1
24-26	Nominal Value	-	-	2.19	16.50	27.90	-	1.99	14.00	-	-	-
	Initial	24.9	999.8	1.97	16.54	25.2	77.4	1.87	13.5	25.30	25.29	
	TC30	24.6	1000.6	1.96	16.56	25	77.2	1.85	13.5	25.07	25.07	-0.8
	TC100	25	1000.4	1.96	16.54	24.9	77	1.85	13.48	24.97	25.01	-1.1
24-27	Nominal Value	-	-	0.40	16.50	5.10	-	0.36	14.00	-	-	-
	Initial	25	999.9	0.34	15.64	4.2	78.8	0.32	12.99	4.20	4.15	
	TC30	25.2	1000.6	0.33	15.7	4.1	78.6	0.31	13.1	4.10	4.12	-0.8
	TC100	25	1000.6	0.33	15.67	4	77.3	0.31	13	4.00	4.05	-2.5
24-28	Nominal Value	-	-	0.46	20.40	6.75	-	0.41	16.50	-	-	-
	Initial	24.9	999.9	0.4	20.51	6.2	75.2	0.37	16.66	6.20	6.21	
	TC30	24.9	1000.6	0.4	20.45	6.1	75.2	0.37	16.6	6.10	6.12	-1.5
	TC100	24.9	1000.6	0.4	20.43	6.1	75.2	0.37	16.58	6.10	6.10	-1.7
24-29	Nominal Value	-	-	0.46	20.40	6.75	-	0.41	16.50	-	-	-
	Initial	25.2	999.9	0.43	20.92	6.8	75.4	0.4	17.06	6.80	6.76	
	TC30	24.9	1000.7	0.42	20.9	6.7	75.3	0.39	17.04	6.71	6.68	-1.2
	TC100	24.7	1000.5	0.42	20.88	6.7	75.3	0.39	17.01	6.71	6.66	-1.6
24-30	Nominal Value	-	-	-	-	8.40	-	0.56	15.24	-	-	-

	Initial	24.7	999.7	0.53	17.14	5.9	64.7	0.45	13.13	5.90	5.92	
	TC30	24.9	1000.4	0.46	17.15	4.9	62.2	0.36	13.44	4.91	4.90	-17.1
	TC100	25.4	1000.4	0.35	17.14	4	66.6	0.28	13.95	4.01	3.96	-33.0

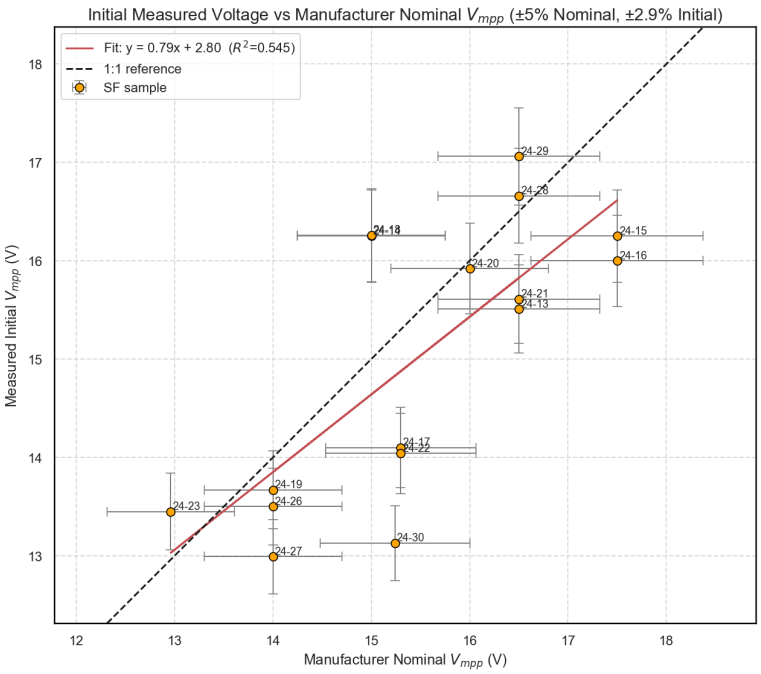

Figure 31 - Phase 2 Vmpp comparison of measured values vs nominal manufacturer values provided

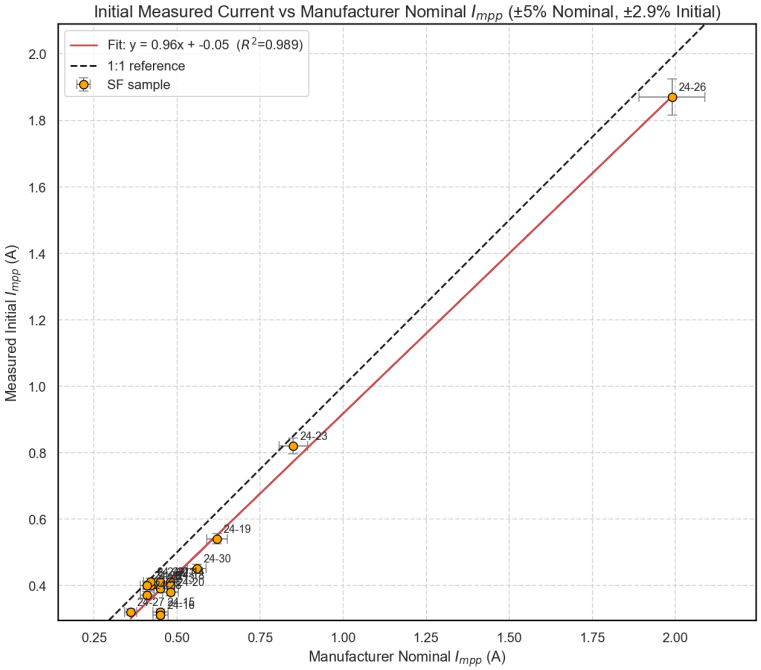

Figure 32 Phase 2 Impp comparison of measured values vs nominal manufacturer values provided

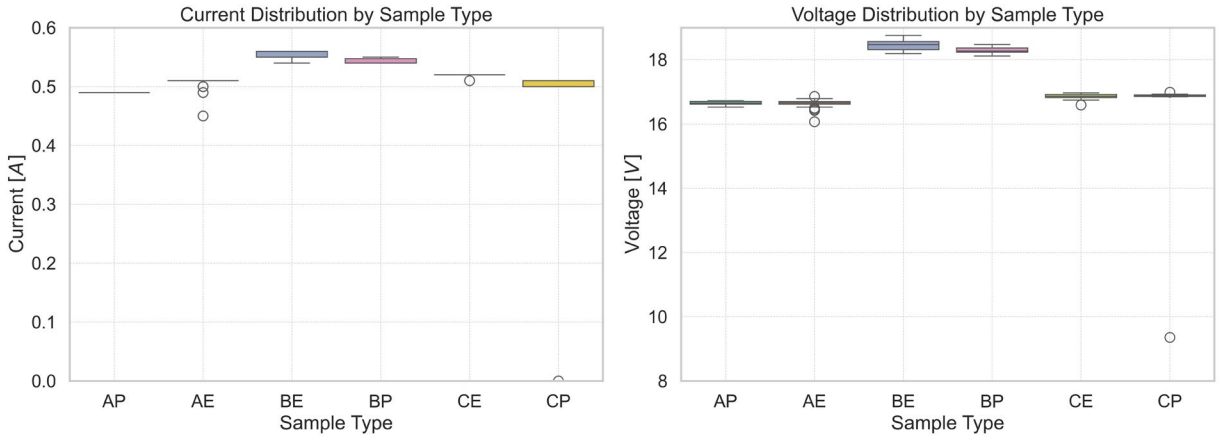

Figure 33 Additional boxplot showing CP-03 sample with no current (0 A) and 9.36 V recorded